CMS-SUS-18-004

Search for supersymmetry in final states with two or three soft leptons and missing transverse momentum in proton-proton collisions at $\sqrt{s} = 13\,\text{TeV}$

The CMS Collaboration*

Abstract

A search for supersymmetry in events with two or three low-momentum leptons and missing transverse momentum is performed. The search uses proton-proton collisions at $\sqrt{s} = 13\,\text{TeV}$ collected in the three-year period 2016–2018 by the CMS experiment at the LHC and corresponding to an integrated luminosity of up to $137\,\text{fb}^{-1}$. The data are found to be in agreement with expectations from standard model processes. The results are interpreted in terms of electroweakino and top squark pair production with a small mass difference between the produced supersymmetric particles and the lightest neutralino. For the electroweakino interpretation, two simplified models are used, a wino-bino model and a higgsino model. Exclusion limits at 95% confidence level are set on $\widetilde{\chi}_2^0/\widetilde{\chi}_1^\pm$ masses up to $275\,\text{GeV}$ for a mass difference of $10\,\text{GeV}$ in the wino-bino case, and up to $205\,(150)\,\text{GeV}$ for a mass difference of $7.5\,(3)\,\text{GeV}$ in the higgsino case. The results for the higgsino are further interpreted using a phenomenological minimal supersymmetric standard model, excluding the higgsino mass parameter μ up to $180\,\text{GeV}$ with the bino mass parameter M_1 at $800\,\text{GeV}$. In the top squark interpretation, exclusion limits are set at top squark masses up to $540\,\text{GeV}$ for four-body top squark decays and up to $480\,\text{GeV}$ for chargino-mediated decays with a mass difference of $30\,\text{GeV}$.

*See Appendix A for the list of collaboration members

1 Introduction

Numerous searches for physics beyond the standard model (SM) at the CERN LHC target weakly interacting massive particles (WIMPs) as potential candidates to explain the nature of dark matter (DM). These WIMPs are predicted to be produced either directly through the interaction of SM particles or indirectly through the decays of new particles with higher mass. Stable WIMPs would escape undetected, yielding a characteristic signature of significant missing transverse momentum (p_T^{miss}) together with any energetic leptons, photons and hadronic jets produced in the cascade of the decaying higher-mass states. In scenarios where the WIMP is the lightest among new particles with a nearly degenerate mass spectrum, the production of these new particles leads to events with relatively low visible energy, and by inference, also low p_T^{miss}. These scenarios are referred to as compressed mass spectra.

Among theories beyond the SM, Supersymmetry (SUSY) [1–5] is particularly attractive owing to the fact that it can provide answers to questions unanswered in the context of the SM, such as the naturalness of the theory [6–8] and the nature of DM. In models where *R*-parity conservation is imposed [9], SUSY particles can only be produced in pairs, and each of their decay chains must lead to the lightest SUSY particle (LSP), which has to be stable. In many models this corresponds to the lightest neutralino ($\widetilde{\chi}_1^0$), a neutral and stable WIMP, which is thus a viable DM candidate [10]. As indicated in several studies, such as in Refs. [6–8, 11–15], naturalness imposes constraints on the masses of higgsinos, top squarks, and gluinos, placing them potentially within the reach of the experiments at the LHC.

Despite numerous searches for new particles, no experimental evidence for their production in LHC collisions has been found, and strong experimental constraints on the masses of SUSY particles have been set. As a result, the relevance of SUSY at the electroweak scale has come under intense scrutiny and several possibilities of how electroweak-scale SUSY might have escaped detection are being considered. Compressed mass spectra offer a possible scenario in which low-energy SUSY might have eluded experiments thus far, if the new particles exist in a region of SUSY parameter space where experimental searches have lower sensitivity.

In compressed spectra scenarios, most of the energy and momentum of higher-mass states is carried away in the rest energy of the LSPs and the remaining detectable SM particles have low momentum. Events with such characteristics can be distinguished from bulk SM processes by requiring a jet with large transverse momentum (p_T) from initial state radiation (ISR) that leads to a large boost of the SUSY particle pair and thus large p_T^{miss}. Final states with only soft jets and moderate p_T^{miss} do not exhibit high sensitivity to new physics because of the presence of huge backgrounds from quantum chromodynamics (QCD) multijet production and Z+jets events with invisible Z boson decays. In the latter case, the SM background can be reduced effectively with the additional requirement of two or three soft light leptons (electrons or muons).

These soft leptons, along with moderate or large p_T^{miss}, constitute the signature of the search presented in this paper. Specifically, the production of charginos ($\widetilde{\chi}_1^\pm$) and neutralinos ($\widetilde{\chi}_1^0$) with nearly degenerate mass, decaying to soft leptons and p_T^{miss} is considered. In what follows, neutralinos and charginos are collectively referred to as electroweakinos.

The results are interpreted in the context of *R*-parity conserving SUSY. A simplified wino-bino model is probed. In such scenarios the LSP can be a WIMP DM candidate that was depleted in the early universe through co-annihilation processes to match the observed DM density [16, 17]. Light higgsinos, which are favored by naturalness arguments, are likely to be nearly degenerate in mass [18–21]. Two minimal SUSY SM (MSSM) hypotheses, where the lightest electroweakinos are higgsino-like, are tested: a simplified higgsino model and a phenomeno-

logical MSSM higgsino model based on the pMSSM [22]. The search is also sensitive to top squark pair production models where a light top squark and the LSP are nearly degenerate in mass and the top squark decays directly to four fermions. The near-degeneracy in mass of the top squark and the LSP is a typical example of the so-called co-annihilation region, in which the LSP is the sole source of DM [23].

Results of searches in final states with soft leptons and missing transverse momentum were previously presented by ATLAS and CMS using data sets at center of mass energy 8 and 13 TeV [24–28]. The previous iteration of this CMS analysis targeted signal events with moderate or large p_T^{miss}, by requiring an ISR jet and a pair of soft oppositely charged (opposite sign (OS)) leptons. The analysis presented in this paper extends the previous search with the addition of soft trilepton final states, as well as a relaxed selection on the dilepton invariant mass (from 4 to 1 GeV) and reoptimized signal regions, yielding extended sensitivity towards lower values of the $\widetilde{\chi}_2^0$-$\widetilde{\chi}_1^0$ mass difference (Δm), where $\widetilde{\chi}_2^0$ is the next to lightest neutralino. The analysis also employs improved methods for the estimation of the nonprompt lepton background and uses the CMS data set collected during 2016–2018, corresponding to an integrated luminosity of up to 137 fb^{-1}. The final results are extracted from a simultaneous binned maximum likelihood fit to the data of the signal and background expectations from all the signal and control regions. The experimental and theoretical uncertainties affecting the background and signal estimations are incorporated as nuisance parameters. The results of this analysis are included in tabulated form in the HEPData record [29].

The paper is organized as follows: Section 2 summarizes the general features of the CMS detector, while Section 3 describes the data set and simulation samples used in this search. After defining the physics objects in Section 4, the event selection and the signal regions of the search are described in Section 5. The background estimation and the systematic uncertainties are discussed in Sections 6 and 7, respectively. The results of the search are presented in Section 8 and their interpretations in the relevant SUSY scenarios in Section 9. The summary of the paper is given in Section 10.

2 The CMS detector

The central feature of the CMS apparatus is a superconducting solenoid of 6 m internal diameter, providing a magnetic field of 3.8 T. Within the solenoid volume are a silicon pixel and strip tracker, a lead tungstate crystal electromagnetic calorimeter (ECAL), and a brass and scintillator hadron calorimeter (HCAL), each composed of a barrel and two endcap sections. Forward calorimeters extend the pseudorapidity (η) coverage provided by the barrel and endcap detectors. Muons are detected in gas-ionization chambers embedded in the steel flux-return yoke outside the solenoid. Events of interest are selected using a two-tiered trigger system. The first level, composed of custom hardware processors, uses information from the calorimeters and muon detectors to select events at a rate of around 100 kHz within a fixed latency of about 4 μs [30]. The second level, known as the high-level trigger, consists of a farm of processors running a version of the full event reconstruction software optimized for fast processing, and reduces the event rate to around 1 kHz before data storage [31].

A more detailed description of the CMS detector, together with a definition of the coordinate system used and the relevant kinematic variables, can be found in Ref. [32].

3 Data and simulated samples

The data used in this search have been collected by the high-level trigger system using three different algorithms (trigger paths): First, an inclusive trigger path requiring the selected events to have online $p_T^{miss} > 120\,\text{GeV}$, where p_T^{miss} is the missing transverse momentum, corrected to account for the contribution of muons. Second, a trigger path that requires at least two muons in addition to p_T^{miss}, with a lower online threshold $p_T^{miss} > 60\,\text{GeV}$. This trigger path also requires the online raw p_T^{miss}, i.e. not corrected for the presence of muons, to be greater than $50\,\text{GeV}$, the p_T of each muon to satisfy $p_T > 3\,\text{GeV}$, and the invariant mass of the muon pair to be between 3.8 and $56\,\text{GeV}$. As this last requirement becomes limiting for events used in the WZ-enriched region of the analysis (defined in Section 6), a third trigger path, with a requirement only on the p_T of the highest p_T muons ($p_T(\ell_1) > 17\,\text{GeV}$ and $p_T(\ell_2) > 8\,\text{GeV}$), is also used. Some of the trigger requirements affect the event selection, e.g., the relaxed selection of the dilepton invariant mass. This is discussed in greater detail in Section 5.

The data sample collected with the inclusive p_T^{miss} trigger corresponds to the total integrated luminosity of each year ($35.9\,\text{fb}^{-1}$ in 2016, $41.5\,\text{fb}^{-1}$ in 2017, and $59.7\,\text{fb}^{-1}$ in 2018). The luminosity that corresponds to the dimuon-only trigger path is slightly lower in 2017 ($36.7\,\text{fb}^{-1}$), while it is slightly lower for the dimuon+p_T^{miss} trigger path in all years ($33.2\,\text{fb}^{-1}$ in 2016, and $59.2\,\text{fb}^{-1}$ in 2018), due to the fact that the trigger paths were disabled for some runs.

Simulated signal and major background processes, such as $t\bar{t}$, DY, W+jets, and Z+jets are generated with the MADGRAPH5_aMC@NLO [33, 34] event generator at leading order (LO) precision in perturbative QCD, with the MLM merging scheme [35] used to consolidate additional partons from the event generator with parton shower generator. The diboson processes WW, ZZ, and Wγ are generated with the same event generator as above at next-to-LO (NLO) precision using the FxFx merging scheme [34], while the WZ process is generated at NLO with POWHEG v2.0 [36–40]. Rare background processes (e.g., $t\bar{t}$W, $t\bar{t}$Z, WWW, ZZZ, WZZ, and WWZ) are also generated at NLO precision with MADGRAPH5_aMC@NLO [33, 34]. The rare background from single top quarks produced in association with a W boson is generated at NLO precision with POWHEG v1.0 [41]. The MADGRAPH5_aMC@NLO versions used are the 2.2.2 (2.3.2 for $t\bar{t}$Z) for 2016 and 2.4.2 (2.6.5 for $t\bar{t}$Z) for 2017 and 2018. The NNPDF3.0 [42] (2016) or NNPDF3.1 [43] (2017 and 2018) LO and NLO parton distribution functions (PDF) are used for the simulated samples generated at LO and NLO respectively. Showering, hadronization, and the underlying event description are carried out using the PYTHIA 8.212 package [44] with the CUETP8M1 (CP5) underlying event tune for 2016 [45, 46] (2017 and 2018 [47]). A detailed simulation of the CMS detector, based on the GEANT4 [48] package, is performed.

The five signal models considered in this analysis include the production of electroweakinos and top squark pairs. Simplified models [49–51] are used in which all SUSY particles other than the electroweakinos (or the top squarks) under study are assumed to be too massive to affect the analysis observables. Such models target scenarios with a bino LSP and wino next-to-LSP (NLSP), a higgsino LSP, and top squarks decaying to electroweakino LSPs. In all of the simplified models in this search, the assumption of 100% branching fractions to a single, representative decay is made. A pMSSM-inspired model is also considered and is described below. Figure 1 shows representative diagrams for simplified models of electroweakino and top squark pair production.

In the wino-bino simplified model (denoted as TCHIWZ), the neutralino-chargino ($\widetilde{\chi}_2^0$-$\widetilde{\chi}_1^\pm$) pair production process is studied assuming a pure wino production cross section, where the $\widetilde{\chi}_2^0$ and $\widetilde{\chi}_1^\pm$ are assumed to be mass degenerate and taken to decay to the LSP via virtual Z and W
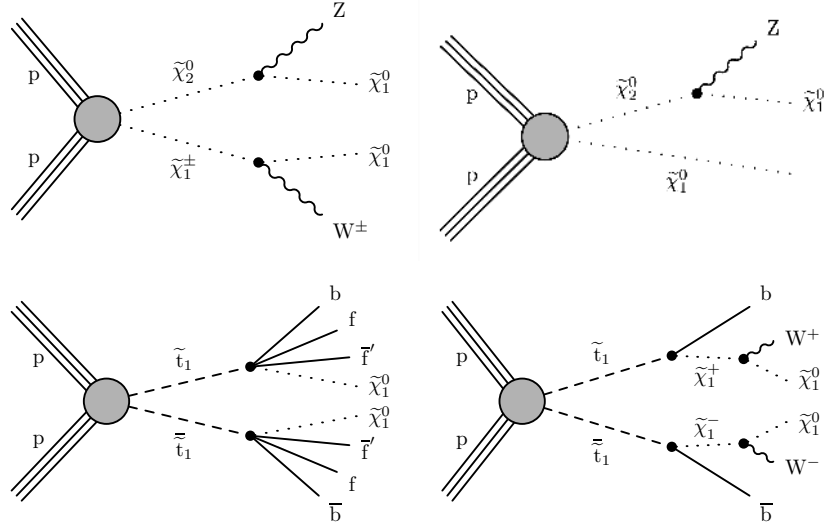
Figure 1: Production and decay of electroweakinos in the TCHIWZ model (upper left), in the higgsino simplified model (upper left and right), in the T2Bff$\widetilde{\chi}_1^0$ model (lower left) and in the T2BW model (lower right).

bosons. For the higgsino simplified model, production through both $\widetilde{\chi}_2^0\widetilde{\chi}_1^{\pm}$ and $\widetilde{\chi}_2^0\widetilde{\chi}_1^0$ channels is considered and $m_{\widetilde{\chi}_1^{\pm}} = \frac{1}{2}(m_{\widetilde{\chi}_1^0} + m_{\widetilde{\chi}_2^0})$ is assumed. In each case, the production cross sections are computed at NLO plus next-to-leading logarithmic (NLL) precision [52–54] and correspond to the cases of pure wino and pure higgsino states, respectively. Mass differences between the $\widetilde{\chi}_2^0$ and $\widetilde{\chi}_1^0$ ranging from 1 to 50 GeV are considered in these simplified models of electroweakino production.

A model inspired by the pMSSM is used for further interpretations in the case of a higgsino LSP. For a higgsino LSP in the pMSSM, the physical mass eigenstates of the $\widetilde{\chi}_1^0$, $\widetilde{\chi}_1^{\pm}$, and $\widetilde{\chi}_2^0$ are determined primarily by the higgsino, bino, and wino mass parameters (μ, M_1, and M_2, respectively) through the neutralino and chargino mixing matrices. The residual dependence on the ratio of the two vacuum expectation values $\tan\beta$ of the Higgs fields is small when $\tan\beta$ is relatively large; here, $\tan\beta$ is fixed to 10. In this model, μ is scanned from 100 to 240 GeV and M_1 from 0.3 to 1.2 TeV with the electroweakino masses and branching fractions calculated from the prescribed pMSSM parameters. The choice of parameters in the scan translates to values for the $\widetilde{\chi}_2^0$-$\widetilde{\chi}_1^0$ mass difference that range from 4 to 28 GeV. In the scan, trilinear couplings are removed and the gluino mass parameter M_3 is assumed to be sufficiently high to decouple from the observable phenomena. The unification-inspired relation $M_1 = 0.5M_2$ is further assumed, in order to reduce the parameter space to a two-dimensional scan. Cross sections are independently calculated for each model point in the pMSSM space using the PROSPINO2 computational package [55]. The SUSY parameters are used to calculate the physical mass spectra and decay rates via additional computational tools [56–60].

Electroweakino decays are implemented using PYTHIA, and are reweighted to incorporate further modeling improvements with respect to Ref. [25]: the dilepton mass spectrum is reproduced from the matrix element and depends on the sign of the product of the two smallest (in magnitude) eigenvalues of the diagonalized neutralino mass matrix [61], denoted as $\widetilde{m}_{\widetilde{\chi}_2^0}$, $\widetilde{m}_{\widetilde{\chi}_1^0}$. While this product is always negative for a higgsino LSP, both cases are possible in the simplified wino-bino model and each is separately considered, since it leads to slightly different invariant mass distributions for the final state leptons. The branching fractions of highly

virtual W and Z bosons to leptons are corrected for massive decay products, as functions of the electroweakino mass splittings, using the SUSY-HIT 1.5a computational package [59].

Finally, two simplified models are considered for top squark pair production. The first model, denoted by T2Bff$\widetilde{\chi}_1^0$ and motivated by Ref. [62], considers the scenario of a top squark NLSP that decays via an off-shell top quark undergoing the four-body process $\widetilde{t} \to b f \overline{f} \widetilde{\chi}_1^0$, where the f and $\overline{f}$ fermions are decay products of the virtual W. In the second model, denoted by T2BW, each top squark is taken to decay to a bottom quark and a chargino $\widetilde{t} \to b \widetilde{\chi}_1^\pm$, with each $\widetilde{\chi}_1^\pm$ subsequently decaying to the LSP with a 100% branching fraction $\widetilde{\chi}_1^\pm \to W \widetilde{\chi}_1^0$, in which the W boson is always off-shell. This decay dominates in naturalness-inspired models featuring light top squarks and higgsinos where only the chargino-mediated decay is not suppressed by an off-shell top quark. In this simplified model, $m_{\widetilde{\chi}_1^\pm} = \frac{1}{2}(m_{\widetilde{t}} + m_{\widetilde{\chi}_1^0})$ is assumed. For each scenario, a range of top squark and LSP masses are considered with a mass difference ranging from 10 to 80 GeV.

Whereas the full detector simulation is used for the wino-bino and the higgsino simplified models, a fast detector simulation [63, 64] is utilized for samples of simulated events for top squark pair production and the pMSSM higgsino model. Typically, in the investigated phase space, the fast detector simulation provides a percent-level agreement with the full detector simulation.

The trigger, lepton identification, and b tagging efficiencies, as well as the distribution of pileup interactions (PU) are corrected in the simulation with scale factors measured in dedicated data samples [65]. Corrections for the use of the fast detector simulation are also applied to the top squark pair production and the pMSSM higgsino signal samples.

4   Object reconstruction

Vertices are reconstructed from tracks according to the deterministic annealing algorithm [66]. The candidate vertex with the largest value of summed physics-object p_T^2 is taken to be the primary pp interaction vertex (PV). The physics objects are the jets, clustered using the jet finding algorithm [67, 68] with the tracks assigned to candidate vertices as inputs, and the associated p_T^{miss}, taken as the negative vector sum of the p_T of those jets. The PV must lie within 24 cm in the z axis direction and 2 cm in the transverse direction from the nominal interaction point. Vertices other than the PV are associated with either PU interactions or with the decay of particles with nonnegligible lifetime (e.g., bottom quarks). The PV is then used in association with the charged-hadron subtraction algorithm [69, 70] to mitigate the effects of pileup in this analysis.

Events are reconstructed using the particle-flow (PF) algorithm [71], which significantly improves the event description, reconstructing and identifying final-state particles by combining information gathered from the entirety of the CMS detector. The energy of photons is obtained from the ECAL measurement. The energy of electrons is determined from a combination of the electron momentum at the PV, as determined by the tracker, the energy of the corresponding ECAL cluster, and the energy sum of all bremsstrahlung photons spatially compatible with originating from the electron tracks. The muon tracks are built by the combination of measurements in the tracker and muon chambers. The momentum of a muon is obtained from the curvature of the corresponding tracks. The energy of charged hadrons is determined from a combination of their momentum measured in the tracker and the matching ECAL and HCAL energy deposits, corrected for the response function of the calorimeters to hadronic showers.

Finally, the energy of neutral hadrons is obtained from the corresponding corrected ECAL and HCAL energies.

The electron momentum is estimated by combining the energy measurement in the ECAL with the momentum measurement in the tracker. It is generally better in the barrel region ($|\eta| < 1.48$) than in the endcaps ($1.48 < |\eta| < 2.50$), and also depends on the bremsstrahlung energy emitted by the electron as it traverses the material in front of the ECAL [72]. Muons are measured in the range $|\eta| < 2.4$. Matching muons to tracks measured in the silicon tracker results in a relative muon p_T resolution of 1% in the barrel and 3% in the endcaps [73] for p_T up to 100 GeV.

In the current analysis, which targets the compressed region of SUSY parameter space, the final-state leptons tend to be soft: the lower p_T threshold of the electrons (muons) is set as low as 5.0 (3.5) GeV. Only soft leptons with p_T up to 30 GeV are used in this analysis.

To identify electrons, a multivariate discriminant based on the energy distribution in the ECAL shower and track quality variables is used. Electrons must be built from tracks that have a hit at every pixel detector layer and are not associated to a conversion vertex. These requirements suppress backgrounds arising from misreconstruction or photon conversions. The identification criteria applied on the muons are based on the quality of the track in the muon system and/or the track in the tracker, and correspond to the loose and soft identification criteria of Ref. [73].

Leptons must be isolated according to the absolute and relative isolation variables. The former counts the energy sum deposited by PF candidates in a cone of radius $\Delta R = 0.3$ around the lepton, where $\Delta R = \sqrt{(\Delta\eta)^2 + (\Delta\phi)^2}$, and ϕ is the azimuthal angle measured in radians. The latter isolation variable is obtained by dividing the absolute isolation by the lepton candidate p_T. The relative isolation criterion is chosen to be rather loose (less than 0.5) in order to ensure a high selection efficiency for soft leptons, while the added absolute isolation requirement is useful for candidates with higher p_T. To mitigate the effect of PU, only charged PF candidates with tracks associated to the PV are considered in the computation of the isolation.

Tight three-dimensional impact parameter requirements are imposed on the leptons [74] to ensure that they are prompt, meaning that they originate from the PV. Leptons are selected only if they satisfy $\mathrm{IP_{3D}} < 0.01$ cm with a significance < 2, where $\mathrm{IP_{3D}}$ is the 3D distance of the lepton from the PV.

The lepton reconstruction, identification, and selection efficiencies depend on the lepton p_T and are different for electrons and muons. For electrons, the efficiency increases with p_T, starting from $\sim$30% at 5 GeV and increasing to $\sim$70% at 30 GeV. For muons, the p_T dependence is less strong and the efficiency ranges from 70 to 85%.

Jets are reconstructed using the anti-k_T algorithm [67] with a distance parameter $R = 0.4$. Tracks from charged particles not associated with the PV are removed from the clustering. Each jet is required to have $p_T \geq 25$ GeV and to be located within the tracker acceptance ($|\eta| < 2.4$). In what follows, the scalar sum of all selected jets is referred to as the transverse hadronic energy, H_T. The energy of the jets is calibrated by correcting for PU effects, the detector response and residual differences between data and simulation [75]. The corrections are verified using data in dijet and Z/photon+jet events [76], exploiting the conservation of momentum in the transverse plane.

A jet tagged as originating from the hadronization of a bottom quark is referred to as b-tagged jet. The identification is achieved using the DEEPCSV flavor tagging discriminant which com-

bines secondary vertex and track-based information into a deep neural network [65]. The medium working point, which is used in this analysis, corresponds to an efficiency of about 68% for a mistagging rate for light flavor quark and gluon jets of approximately 1%.

The raw p_T^{miss} is defined as the magnitude of the negative vector p_T sum of all PF candidates reconstructed in the event [77], corrected by propagating the jet calibration corrections presented above. In this analysis we apply a further correction to account for the presence of muons, with the goal of matching more closely the definition used in the trigger system. We define the resulting variable as p_T^{miss}.

Anomalous high-p_T^{miss} events can be present due to a variety of reconstruction failures, detector malfunctions, or noncollision backgrounds. Such events are rejected by event filters that are designed to identify more than 85–90% of the spurious high-p_T^{miss} events with a mistagging rate of less than 0.1% [77].

5 Event selection

The analysis requires events with a distinct signature of two or three leptons with low p_T, forming at least one OS pair and significant p_T^{miss} induced by an ISR jet.

The search regions (SRs) are defined in bins of raw p_T^{miss} and p_T^{miss} (for simplicity referred to as MET bins), with boundaries selected such that in each bin high efficiency and stable online selection are ensured by either the p_T^{miss} or the dimuon+p_T^{miss} trigger path. The MET binning of the analysis is presented in Table 1. Four MET bins are defined for the SRs that target signal events with electroweakinos (Ewk) that decay into final states with 2 leptons (2ℓ-Ewk). Only two MET bins are considered for signal events with three leptons in the final state (3ℓ-Ewk). For signal events with top squarks (2ℓ-Stop) the upper boundaries of the MET bins are higher by 50 GeV, to increase the sensitivity of the search.

Table 1: Definition of the MET bins of the SRs. The boundaries of raw p_T^{miss} and p_T^{miss} (in GeV) of every bin are described.

Search region	Low-MET		Med-MET	High-MET	Ultra-MET
	Raw p_T^{miss}	p_T^{miss}	p_T^{miss}	p_T^{miss}	p_T^{miss}
2ℓ-Ewk	> 125	$(125, 200]$	$(200, 240]$	$(240, 290]$	> 290
2ℓ-Stop	> 125	$(125, 200]$	$(200, 290]$	$(290, 340]$	> 340
3ℓ-Ewk	> 125	$(125, 200]$		> 200	

Each MET bin is further categorized by a specific discriminating variable. In the 2ℓ-Ewk SRs, the dilepton invariant mass $M(\ell\ell)$ of a pair of OS same flavor (SF) leptons, $(M_{SFOS}(\ell\ell))$, is used as it has an endpoint at the mass difference of $\widetilde{\chi}_2^0$-$\widetilde{\chi}_1^0$. In the 3ℓ regions, the minimum of the invariant masses, $(M_{SFOS}^{min}(\ell\ell))$, is used as the binning variable, since we expect our signal to have small mass differences.

The $M(\ell\ell)$ binning used in the low-MET bin is [4, 10, 20, 30, 50] GeV, where the lowest boundary at 4 GeV is set due to the dimuon+p_T^{miss} trigger requirements described in Section 3. Because of the requirements of this trigger, only $\mu\mu$ pairs are used in the low-MET bin. In the medium-, high- and ultra-MET bins, where the pure p_T^{miss} trigger is used, the lowest $M(\ell\ell)$ boundary is relaxed to 1 GeV and the binning is [1, 4, 10, 20, 30, 50] GeV. Dielectron pairs are also accepted in these bins.

In the 2ℓ-Stop SR, the leptons are not bound to have same flavor (except for the low-MET bin, where again only $\mu\mu$ pairs are allowed due to the trigger requirements mentioned above) and

their $M(\ell\ell)$ spectrum has no sharp endpoint. The binning in this case is applied on the p_T of the leading lepton, with boundaries [3.5, 8, 12, 16, 20, 25, 30] GeV.

Table 2 summarizes the event selection criteria applied in the three SR groups, i.e. 2ℓ-Ewk, 2ℓ-Stop and 3ℓ-Ewk, respectively. The selection requirements based on lepton quantities are shown in the upper part of Table 2. Further requirements on the topology of the event are applied as listed in the lower part of Table 2. The motivations for some of the requirements are presented below:

- An Y-meson veto and a J/ψ-meson veto are applied by rejecting events with $M(\ell\ell)$ in the [9, 10.5] and [3, 3.2] GeV ranges respectively.

- $H_\mathrm{T} > 100$ GeV suppresses background events with low hadronic activity.

- $2/3 < (p_\mathrm{T}^\mathrm{miss}/H_\mathrm{T}) < 1.4$ in the dilepton final state selection is found to suppress effectively QCD multijets events, while retaining signal events boosted by ISR.

- The requirement of "tight lepton veto" [78] identification criteria for the leading jet, which removes jets from calorimetric noise as well as jets from misreconstructed leptons, in combination with the sizable H_T required, can only be realized by a jet coming from the initial state (ISR jet). This is because there is no photon or gluon final state radiation (FSR) from the LSP, which is neutral and not strongly interacting. Moreover, since the emitted SM particles and their subsequent decay products are off-shell and soft, due to the small ΔM of the signal, potential FSR from those particles or the jets from the hadronic decay of the W are going to have low p_T, which is much lower than the H_T required for the event selection. Finally, events with high multiplicity of soft jets that could potentially add up to 100 GeV of H_T are very unlikely.

- Leptonic W boson decays in $t\bar{t}$ events can yield two prompt leptons and b-tagged jets in the final state. The $t\bar{t}$ background is suppressed by vetoing events with b-tagged jets with p_T above 25 GeV. Events containing softer jets from the fragmentation and hadronization of a bottom quark are still retained, e.g., in the case of the top squark decay in T2bff$\widetilde{\chi}_1^0$ and T2bW models.

- The contamination from Drell–Yan (DY) events can be reduced significantly by applying a selection on the approximate invariant mass of the Z boson. Lorentz-boosted Z bosons that decay into two τ leptons, which further decay into two leptons and four neutrinos, can satisfy the event selection requirements. In such decays, the momentum direction of the final leptons is close to the original momentum direction of the Z boson. The momenta of the leptons are rescaled to balance the hadronic recoil of the Z boson, thus yielding an estimate of the transverse momenta of the two τ leptons. These are then used to estimate the invariant mass of the two τ leptons, $M_{\tau\tau}$ [79]. The range $0 \leq M_{\tau\tau} \leq 160$ GeV is vetoed, since it is found to contain most of the DY events and negligible contributions from signal events. Negative values of $M_{\tau\tau}$ correspond to the cases when the momentum of either lepton flips direction during rescaling.

- The requirement on the transverse mass between each lepton and $p_\mathrm{T}^\mathrm{miss}$, $m_\mathrm{T}(\ell_i, p_\mathrm{T}^\mathrm{miss})$ $(i = 1, 2)$, to be less than 70 GeV, has been found to be effective in reducing the $t\bar{t}$ background, the scale being set by the W boson mass. It is not applied in the 2ℓ-Stop SRs in order to increase the stop signal acceptance.

Table 2: List of all criteria that events must satisfy to be selected in one of the SRs. The label "Low-MET" refers to the low-MET bin of the analysis, while the label "Higher-MET" refers collectively to the Med-, High- and Ultra-MET bins of the analysis.

Variable	2ℓ-Ewk		2ℓ-Stop		3ℓ-Ewk	
	Low-MET	Higher-MET	Low-MET	Higher-MET	Low-MET	Higher-MET
N_{lep}	2	2	2	2	3	3
$p_T(\ell_1)$ [GeV] for e(μ)	$(5, 30)$	$(5, 3.5), 30)$	$(5, 30)$	$(5, 3.5), 30)$	$(5, 30)$	$(5, 3.5), 30)$
$p_T(\ell_2)$ [GeV] for e(μ)	$(5, 30)$	$(5, 3.5), 30)$	$(5, 30)$	$(5, 3.5), 30)$	$(5, 30)$	$(5, 3.5), 30)$
$p_T(\ell_3)$ [GeV] for e(μ)	—	—	—	—	$(5, 30)$	$(5, 3.5), 30)$
1 OS pair	✓	✓	✓	✓	✓	✓
1 OSSF pair	✓	✓	✓	—	✓	✓
$\Delta R(\ell_i \ell_j)$ ($i, j = 1, 2, 3, i \neq j$)	—	> 0.3	—	> 0.3	—	> 0.3
$M_{\text{SFOS}}(\ell\ell)$ ($M_{\text{SFOS}}^{\min}(\ell\ell)$ in 3ℓ) [GeV]	$(4, 50)$	$(1, 50)$	$(4, 50)$	$(1, 50)$	$(4, 50)$	$(1, 50)$
$M_{\text{SFAS}}^{\max}(\ell\ell)$ (AS=any sign) [GeV]	—	—			< 60	—
$M_{\text{SFOS}}(\ell\ell)$ ($M_{\text{SFOS}}^{\min}(\ell\ell)$ in 3ℓ) [GeV]			veto $(3, 3.2)$ and $(9, 10.5)$			
$p_T(\ell\ell)$ [GeV]		> 3		> 3		—
Leading jet "Tight lepton veto"		✓		✓		—
$m_T(\ell_i, p_T^{\text{miss}})$ [GeV] ($i = 1, 2$)		< 70		—		—
H_T [GeV]				> 100		
p_T^{miss}/H_T		$(2/3, 1.4)$		$(2/3, 1.4)$		—
$N_b(p_T > 25\,\text{GeV})$				$= 0$		
$M_{\tau\tau}$ [GeV]		veto $(0, 160)$		veto $(0, 160)$		—

6 Background estimation

The residual SM background present in the dilepton and trilepton SRs can be classified into four main categories. Two major backgrounds with prompt leptons arise from DY and $t\bar{t}$ production. A third background arises from diboson production: WW production for dileptons and WZ production for trileptons. A fourth background arises from nonprompt or misidentified leptons, mainly from W+jets events in the dilepton search and mainly from $t\bar{t}$ events in the trilepton search. Finally, rare SM processes lead to minor contributions in all SRs.

For each of the dominant prompt lepton SM backgrounds, a control region (CR) orthogonal to the SRs and enriched in the associated background process is defined. Each CR is split into two MET bins according to raw p_T^{miss} and p_T^{miss} to match the event categorization employed in the search regions:

- Low-MET: Raw $p_T^{\text{miss}} > 125\,\text{GeV}$ and $125 < p_T^{\text{miss}} < 200\,\text{GeV}$;
- High-MET: $p_T^{\text{miss}} > 200\,\text{GeV}$.

In particular, to verify and constrain the modeling of the dominant prompt-lepton backgrounds, two CRs with negligible signal contribution and with very high purity in the DY and $t\bar{t}$ dilepton processes, referred to as the DY and $t\bar{t}$ CRs, are used. Correspondingly, a CR designed to be enriched in trilepton WZ with nonnegligible signal contamination is referred to as the WZ-enriched region. Another CR, with moderate purity targeting dileptons from diboson processes, VV, is introduced and is referred to as the validation region (VR). The $M(\ell\ell)$ distributions from the DY CR, $t\bar{t}$ CR, and WZ-enriched regions are included in the signal extraction procedure, which is based on a maximum likelihood fit to the data, while the VV VR is only used to assess an estimate of the corresponding background normalization uncertainty.

An additional dilepton CR comprising events with same sign (SS) leptons is used to constrain the background from nonprompt or misidentified leptons. This is described in detail in Section 6.6. The SS CR is defined only for $p_T^{\text{miss}} > 200\,\text{GeV}$ (high-MET bin) and cannot be extended to lower p_T^{miss}, due to the opposite-sign requirement of the dimuon+p_T^{miss} trigger. The $M(\ell\ell)$ distributions of this CR are included in the maximum likelihood fit to the data as well.

Table 3 presents the selection criteria for the various background CRs that are modified with respect to those of the SR, described in Table 2.

For each of the DY, $t\bar{t}$, and WZ processes, and for each of the two MET bins, an unconstrained scale factor is included as a nuisance parameter in the maximum likelihood fit, to correct the normalization of the simulation yields of each process to match the data. The uncertainties on the predicted yields include the statistical and systematic components, as described in Section 7.

Table 3: Summary of changes in the selection criteria with respect to the SR for all the background control and validation regions.

Region	Modified selection criteria
DY(2ℓ) CR	$0 < M_{\tau\tau} < 160\,\text{GeV}$ No upper requirement on the lepton p_T
$t\bar{t}$(2ℓ) CR	At least one b-tagged jet with $p_\text{T} > 25\,\text{GeV}$ No requirement on $m_\text{T}(\ell_i, p_\text{T}^\text{miss})$ (instead of $< 70\,\text{GeV}$) No upper requirement on the lepton p_T
VV(2ℓ) VR	$m_\text{T}(\ell_i, p_\text{T}^\text{miss}) > 90\,\text{GeV}$ (instead of $< 70\,\text{GeV}$) No upper requirement on the lepton p_T
WZ(3ℓ) enriched region	No $M_{\text{SFOS}}^{\text{min}}(\ell\ell)$ upper requirement at $50\,\text{GeV}$ No $M_{\text{SFAS}}^{\text{max}}(\ell\ell)$ requirement $p_\text{T}(\ell_1) > 30\,\text{GeV}$ $p_\text{T}(\ell_2) > 10\,\text{GeV}$ ($> 15\,\text{GeV}$ if ℓ is electron in high-MET bin) $p_\text{T}(\ell_3) > 10\,\text{GeV}$ ($> 15\,\text{GeV}$ if ℓ is electron in high-MET bin) At least one μ with $p_\text{T} > 20\,\text{GeV}$
SS(2ℓ) CR	Same-sign requirement on lepton electric charge No requirement on $m_\text{T}(\ell_i, p_\text{T}^\text{miss})$

6.1 DY control region

As explained in Section 5, the reconstructed mass $M_{\tau\tau}$ of the τ pair is used to suppress DY events. The dedicated DY CR is defined by inverting the $M_{\tau\tau}$ requirement, selecting events in the range of 0–160 GeV. Additionally, the 30 GeV upper bound on the lepton p_T is removed. The post-fit distributions of the $M(\ell\ell)$ variable in the DY CRs are shown in Fig. 2. Typical scale factors of 1.2–1.7 for each data set are found between the pre- and post-fit normalizations of the DY background in the low-MET bin, and of 1.2–1.4 in the high-MET bin of the DY CR. The slightly higher deviations from unity with respect to other CRs arise because these factors correct for events that contain large amounts of instrumental p_T^miss, which is typically mismodeled in the simulation.

6.2 $t\bar{t}$ control region

Even though the $t\bar{t}$ background component is significantly suppressed in the search regions by vetoing events containing at least one b-tagged jet, it is the dominant prompt background in the dilepton SRs. For the definition of the dedicated $t\bar{t}$ CR at least one b-tagged jet with $p_\text{T} > 25\,\text{GeV}$ is required, ensuring orthogonality to the SR selection. In addition, the upper bound on the $m_\text{T}(\ell, p_\text{T}^\text{miss})$ for each lepton is removed, and no upper bound on the lepton p_T
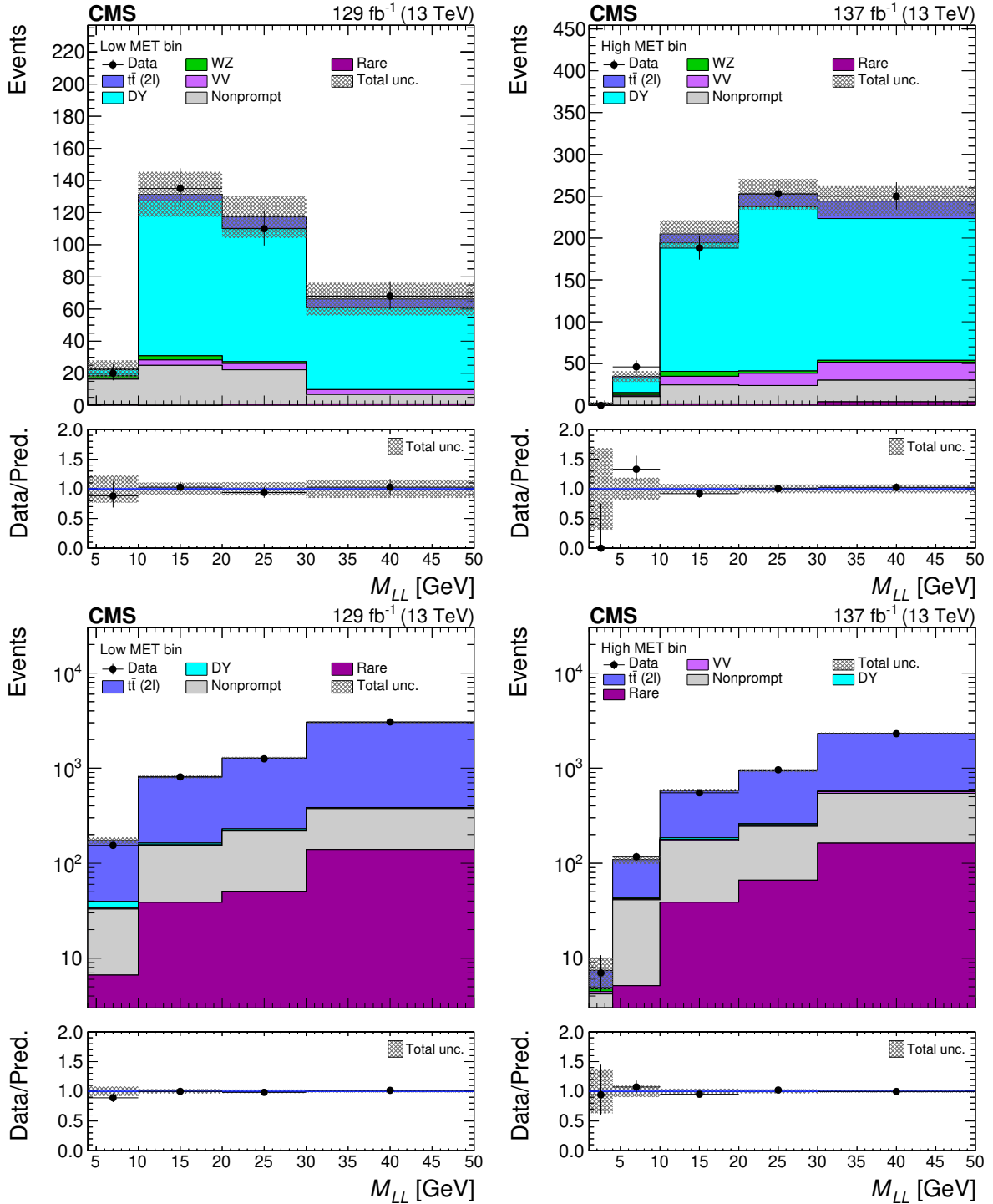
Figure 2: The post-fit distribution of the $M(\ell\ell)$ variable is shown for the low- (left) and high- (right) MET bins for the DY (upper) and tt̄ (lower) CRs. Uncertainties include both the statistical and systematic components.

is applied. The post-fit distributions of the $M(\ell\ell)$ variable are shown in Fig. 2. Typical scale factors of 0.9–1.1 are found for each data set between the pre- and post-fit normalization of the tt̄ background in the low-MET bin, and of 0.8–1.2 in the high-MET bin.

6.3 WZ-enriched region

The decay of bosons in WZ events to three leptons is the dominant prompt background process for the 3ℓ SRs (the WZ label shown in the plots corresponds to W and Z bosons both decaying leptonically while the other decay modes are included in the VV label, described in the next subsection). In order to assess the normalization of the SM WZ process to fully leptonic final states, a WZ-enriched region is employed, split in the same two MET bins as for the other CRs. In the low-MET bin of the WZ-enriched region, a pure dimuon trigger is used instead of the dimuon+$p_{\mathrm{T}}^{\mathrm{miss}}$ one, since the latter includes a requirement on the invariant mass of the two muons. The event selection in the WZ-enriched region differs from the 3ℓ SR event selection in that no upper $M_{\mathrm{SFOS}}^{\min}(\ell\ell)$ selection or $M^{\max}(\ell\ell)$ Z veto is applied. Furthermore, no upper bound on $p_{\mathrm{T}}(\ell)$ is applied, while the lower bounds on $p_{\mathrm{T}}(\ell)$ are set to $p_{\mathrm{T}}(\ell_1) > 30\,\mathrm{GeV}$, $p_{\mathrm{T}}(\ell_2) > 10\,\mathrm{GeV}$ and $p_{\mathrm{T}}(\ell_3) > 10\,\mathrm{GeV}$, requiring at least one muon with $p_{\mathrm{T}} > 20\,\mathrm{GeV}$ as driven by the pure dimuon trigger. The fraction of events from WZ decays in this selection is 78(88)% in the low(high)-MET bin.

When split into the $M(\ell\ell)$ bins, the low-$M(\ell\ell)$ range of the WZ-enriched region could have some nonnegligible signal contribution in the case of intermediate- and higher-mass splittings (30–40 GeV) with respect to the overall WZ process contribution. Therefore, the part of the WZ-enriched region that satisfies $1 < M(\ell\ell) < 30\,\mathrm{GeV}$ contributes to the sensitivity of the analysis and is defined as WZ-like SR. The $M(\ell\ell) > 30\,\mathrm{GeV}$ region, which includes the majority of the WZ process yields, is defined as WZ CR.

The post-fit distributions of the $M(\ell\ell)$ variable are shown in Fig. 3. Typical scale factors of 0.7–0.8 are found for each data set between the pre- and post-fit normalizations of the WZ background in the low-MET bin, and of 0.6–0.8 in the high-MET bin. These scale factors tend to have somewhat large deviations from unity, as they account for the overestimation of the WZ background normalization in the simulation.

6.4 VV validation region

Diboson production VV accounts for the mixture of WW, WZ (all decay modes, except the fully leptonic one), and ZZ events, where the processes are given in descending order with respect to their contribution in the dilepton search regions. The event selection of the VV VR is obtained by inverting the $m_{\mathrm{T}}(\ell_i, p_{\mathrm{T}}^{\mathrm{miss}})$ requirement, removing the upper bound on the lepton p_{T} and requiring a high-p_{T} ($> 30\,\mathrm{GeV}$) leading lepton to ensure orthogonality to the SRs. This region is less pure with respect to the CRs mentioned so far; it has a purity of 18% and 31% for the low-MET and high-MET selection, respectively. It is thus only used to check the pre-fit data and simulation agreement, which is found to be good. This VV-like region is not included in the maximum likelihood fit.

6.5 Rare SM processes

The previously mentioned SM processes leading to minor contributions in the SRs are collectively referred to as rare. These comprise the production of a W, Z or Higgs boson (H) in association with top quarks, such as tW, $t\bar{t}$V, $t\bar{t}$H, tZW, and triboson processes VVV. Due to their very small contribution in the SR, no dedicated CR is designed for the estimation of these processes and their yield is taken directly from simulation.

6.6 Nonprompt background

The background from nonprompt or misidentified leptons is evaluated with the "tight-to-loose" method [80]. For the calculation of the nonprompt background in the SR two additional
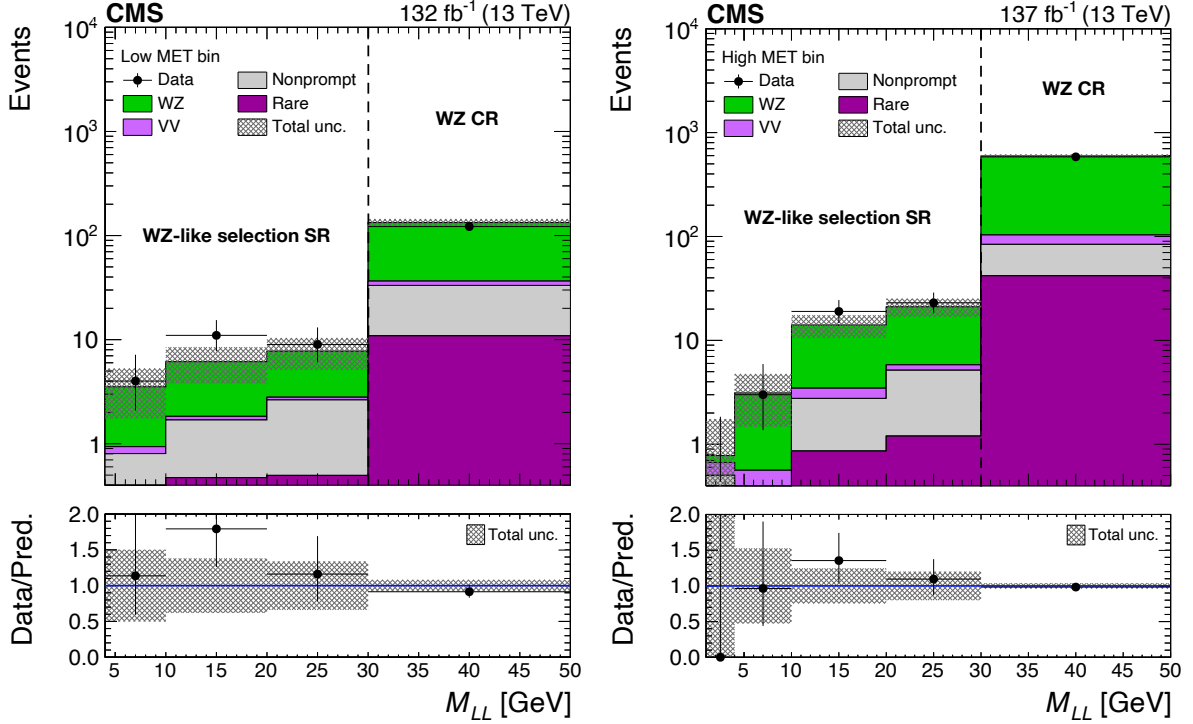
Figure 3: The post-fit distribution of the $M(\ell\ell)$ variable is shown for the low- (left) and high-(right) MET bins for the WZ-enriched region. Uncertainties include both the statistical and systematic components.

regions need to be defined. The application region (AR) is selected by applying the SR requirements except the tight identification and isolation lepton requirement which is replaced by at least one lepton failing the tight identification and isolation criteria but passing a looser selection. Therefore, the AR is enriched in nonprompt leptons. The measurement region (MR) is a region enriched in events that contain strongly produced jets, referred to as QCD multijet events. The MR is defined by requiring one loose lepton, and a jet separated from the lepton by $\Delta R \geq 0.7$. The probability that a nonprompt lepton that passes the loose selection also satisfies the tight selection is called the fake rate and it is measured in MR data as a function of lepton p_{T} and η. The probability of a prompt lepton to pass the tight identification and isolation requirement is called prompt rate and it is measured in simulation. The nonprompt background estimation in the SR is performed by weighting the AR events by a transfer factor (TF), which depends on the fake rate and the prompt rate.

The MR for muons is selected by prescaled single-muon triggers with no isolation requirement, while for electrons, a mixture of prescaled jet triggers is used. The jet selection requirements applied for the MR for muons is $p_{\mathrm{T}} \geq 50\,\mathrm{GeV}$ and for the electrons are $p_{\mathrm{T}} \geq 30(40)\,\mathrm{GeV}$ in 2018 (2016 and 2017), according to the trigger requirements that evolved during data-taking.

In the data-driven tight-to-loose method, the fake rate is measured in QCD multijet data events of the MR and applied in W+jets and $t\bar{t}$ data events with loose leptons in the AR. Therefore, the jet flavor composition of the MR and the AR may differ and this can affect the prediction of the nonprompt background. The fake rate calculated in QCD multijet simulation was studied and found to be consistent across the different processes. The closure of the method is verified by applying the fake rate determined from QCD multijet data events to simulated W+jets and $t\bar{t}$ events containing at least one nonprompt lepton in the AR. The resulting estimated nonprompt background in the SR is compared with the observed simulated W+jets and $t\bar{t}$ events with at

least one nonprompt lepton in the SR. The maximum nonclosure of the method is found to be 40% and this value is used as the systematic uncertainty in the normalization of the nonprompt background.

The TF are constructed with the prompt rate and the fake rate and they are applied on the AR events, in which at least one lepton fails the tight identification and isolation criteria. This yields the number of events with nonprompt leptons in the SR. This method is applied in MET bins with sizable numbers of events, e.g., the low-MET bins of the 2ℓ-Ewk and Stop SRs. In MET bins with limited numbers of events, namely the medium-, high- and ultra-MET bins of the 2ℓ-Ewk and Stop SR and the low- and high-MET bins of the 3ℓ SR, the nonprompt-lepton background is estimated by applying the TF to the $M(\ell\ell)$ shapes in the AR, as obtained by simulation and normalized to data. This latter approach maintains the robustness in the measurement of the misidentification probability by utilizing control samples in data and in the normalization of the misidentified-lepton background in the AR, while using the $M(\ell\ell)$ shape in simulation to reduce statistical fluctuations.

To reduce the statistical uncertainty in the estimation of the nonprompt-lepton background in the 2ℓ-Ewk medium-, high- and ultra-MET SRs, the $M(\ell\ell)$ shape of the nonprompt-lepton simulation in the AR is merged into one inclusive MET bin. The simulated $M(\ell\ell)$ shape of the nonprompt-lepton background is indeed found to be compatible across different MET bins. A dedicated systematic uncertainty is applied to the nonprompt-lepton background in the 2ℓ-Ewk medium-, high- and ultra-MET bins, to account for the $M(\ell\ell)$ shape extrapolation across the MET bins.

The SS CR is used to further constrain the nonprompt-lepton background prediction uncertainty using data. This CR is obtained by requiring two leptons of the same sign instead of opposite sign when applying the 2ℓ-Stop SR selection in the $p_{\mathrm{T}}^{\mathrm{miss}} > 200\,\mathrm{GeV}$ region. The requirement of two SS leptons increases significantly the probability that at least one of the two is nonprompt, thus enriching the CR in nonprompt-lepton background. The $M(\ell\ell)$ distribution of the SS CR, with the nonprompt-lepton background predicted with the tight-to-loose method, is included in the maximum likelihood fit. The post-fit $M(\ell\ell)$ distribution of the SS CR is shown in Fig. 4. A scale factor of 1.06 is estimated between the pre- and post-fit normalizations of the tight-to-loose prediction.

7 Systematic uncertainties

Systematic uncertainties arise from experimental effects and from the modeling of the simulated processes. This section describes the sources of systematic uncertainties and quantifies their effect on the estimated background. The post-fit effect of each source of uncertainty is quoted.

All of the trigger, lepton selections, and b tagging efficiency corrections that are applied to simulated samples have uncertainties related to the methods used to estimate them from data; these uncertainties affect the final predictions with values that fall in the ranges 2–9%, 2–9% and 1–4%, respectively. Additional experimental uncertainties arise from the jet energy scale and resolution corrections that account for any differences between data and simulation when measuring the jet energies. These uncertainties affect all simulated backgrounds and result in 1–10% uncertainty in the total background prediction. The uncertainties of the trigger efficiency and lepton selection are applied separately for each year, while the b tagging efficiency and the jet energy corrections are correlated across years and are treated accordingly.
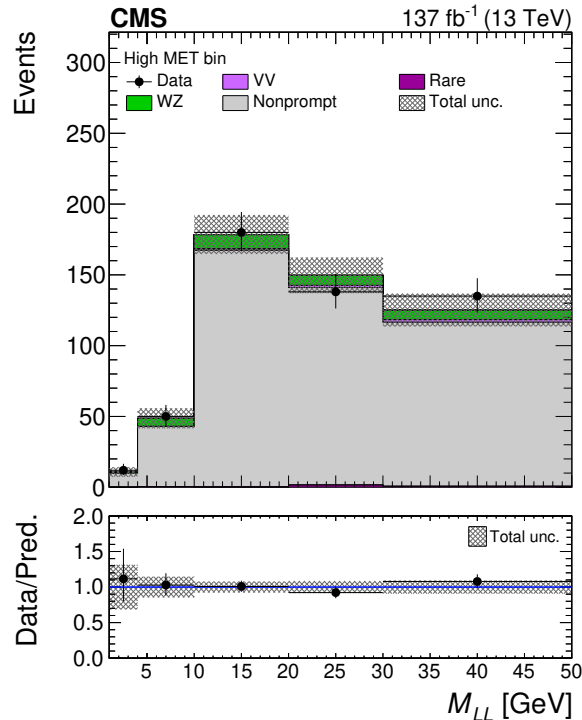
Figure 4: The post-fit distribution of the $M(\ell\ell)$ variable is shown for the high-MET bin for the SS CR. Uncertainties include both the statistical and systematic components.

Dedicated weights are applied to the simulated samples to correct the distribution of the true number of PV to the one measured in data. The number of interactions per bunch crossing is estimated from the total inelastic cross section, which has been measured with an uncertainty of 4.6% [81]. The PU uncertainty is estimated by propagating the total inelastic cross section uncertainty to the PU weights and using their variation as a shape uncertainty for all years combined. The net effect on the final total background prediction is found to be at most 1–2%.

The uncertainties in the luminosity measurements are incorporated in the estimates of all the prompt-lepton backgrounds and the predicted signal yields. These uncertainties are 2.5%, 2.3% and 2.5% for the 2016 [82], 2017 [83], and 2018 [84] data set, respectively, treated as uncorrelated among the different years.

As presented in Section 6, the dedicated CRs for the dominant prompt-lepton backgrounds are included in the maximum likelihood fit to the data. The normalization of each of these processes is left to float freely in the fit, independently for each year and for each MET bin. The resulting uncertainties are found to be in the ranges 15–35% for the DY, ∼15% for the $t\bar{t}$, and 12–27% for the WZ backgrounds.

The VV background, described in Section 6, accounts for all the diboson processes that enter the dilepton search. Its modeling is validated in the VV VR, and its estimated contribution is assigned an uncertainty of 50%, correlated across the three years.

To fully account for all uncertainties related to the simulation of the rare SM processes, a conservative uncertainty of 50% has been assigned to these minor backgrounds for all years.

From the closure tests of the tight-to-loose method, which are presented in Section 6.6, a pre-fit systematic uncertainty of 40%, correlated across the three years of data-taking, is assigned on the misidentified-lepton background estimation. This background, however, is constrained significantly by including the SS CR in a single MET bin ($p_T^{miss} > 200\,\text{GeV}$) in the maximum like-

lihood fit. With the inclusion of the SS CR in the fit, the post-fit uncertainty in the nonprompt-lepton background after the fit is reduced to ∼5%.

An extra shape uncertainty is applied to the nonprompt-lepton background prediction to account for potential disagreements between data distributions and the templates from simulation used in the ARs. An additional shape uncertainty is included for the SRs for which the corresponding AR distributions are merged across MET bins to account for minor shape discrepancies in different MET bins. These shape uncertainties are applied to the nonprompt prediction independently for every year. The post-fit effect of these two separate shape uncertainties on the nonprompt background is approximately 8% and 5%, respectively.

Two additional uncertainties are assigned to all simulated signal samples: The uncertainty in the theoretical cross section due to the variation of the parton density functions is included in the $\pm 1\sigma$ curves on the limit scans, and amounts to 3.5–8.5%. The acceptance uncertainties due to the variations of the renormalization and factorization scales are added separately as nuisance parameters in the maximum likelihood fit and are of ∼1% each.

Potential differences between data and simulation in modeling ISR jets are also a source of systematic uncertainty. To this end, the data are compared with the simulation in a general selection that requires two isolated leptons and at least one ISR jet. The residual differences between data and simulation are used to determine p_T-dependent correction factors, independently for each data-taking year. The correction factors are applied to the simulation and their differences from unity (1–5%) are assigned as a systematic uncertainty.

Differences in the p_T^{miss} reconstruction in the detailed and fast simulations used for the signal samples are taken into account as an additional systematic uncertainty for each year separately. This uncertainty varies between 1 and 10% for the yields of the fast simulation signal samples.

During the 2016 and 2017 data-taking periods, a gradual shift was observed in the timing of the trigger information from the ECAL towards early values. This causes a sizable fraction of electromagnetic objects with $|\eta| > 2.5$ to be assigned to the previous bunch crossing. To account for this issue, correction factors are applied and their uncertainties (∼1%) are propagated to the final result.

The uncertainties presented above are included as nuisance parameters in the likelihood fit to the data. To freely float in the fit, the DY, $t\bar{t}$ and WZ backgrounds are assigned uniformly distributed uncertainties, whereas all other fit parameters are assigned normally distributed uncertainties. The dominant uncertainties are generally the statistical ones. The prompt and nonprompt background normalization uncertainties also become important, depending on the part of the phase space that is probed.

8 Results

The signal and background expectations are fitted to the data using a binned maximum likelihood fit with the uncertainties incorporated as nuisance parameters, as mentioned above. The signal yields are scaled in all regions of the analysis (also in the CRs to account for possible signal contamination) by a single, unconstrained parameter of interest. The CRs for the DY, $t\bar{t}$ and WZ processes are added to determine the normalization of the respective processes. Similarly, the SS dilepton CR is included in the fit in order to constrain the nonprompt background. The distribution that enters the maximum likelihood fit is the $M_{\text{SFOS}}^{\min}(\ell\ell)$ for the 3ℓ CRs and the 3ℓ-Ewk SRs, and the $M(\ell\ell)$ for the 2ℓ CRs and the 2ℓ-Ewk SRs. Each distribution is comprised by 4 bins in the low-MET bins and 5 bins otherwise. For the 2ℓ-Stop SRs, the p_T distribution of

the leading lepton (6 bins in each MET bin) is used. In total, the fit that targets signal models with electroweakinos is given 28 SRs (19 dilepton and 9 trilepton SRs), while for models with top squark production 24 SRs (dilepton only) are used. In both cases, the same 32 CR bins are used.

The estimated yields for the SM background processes and the data observed in the 2ℓ- and 3ℓ-Ewk SRs are shown in Figs. 5 and 6 respectively, while Fig. 7 shows the 2ℓ-Stop SRs. The estimated yields from the different backgrounds and the data are also summarized in Tables 4–7 for each SR. The estimates correspond to the post-fit results (background-only), extracted from the maximum likelihood fit to the data. The uncertainties in the predicted yields include both statistical and systematic components, as described in Section 7. No significant deviation from the SM prediction is observed in the data.

Table 4: Observed and predicted yields as extracted from the maximum likelihood fit, in the 2ℓ-Ewk SRs. Uncertainties include both the statistical and systematic components.

p_T^{miss} [GeV]	$M(\ell\ell)$ [GeV]	t$\bar{\text{t}}$	DY	VV	WZ	Rare	Nonprompt	Total bkg	Data
125–200	4–10	4.0 ± 2.0	20.6 ± 5.2	3.7 ± 2.4	8.3 ± 2.6	$0.28^{+0.72}_{-0.27}$	31.9 ± 5.6	68.7 ± 8.7	73
	10–20	16.5 ± 4.2	28.0 ± 6.2	6.2 ± 3.2	6.5 ± 2.3	2.8 ± 2.1	90.1 ± 9.3	151 ± 13	165
	20–30	18.0 ± 4.4	36.3 ± 7.1	7.8 ± 3.5	3.5 ± 1.7	2.9 ± 2.1	82.1 ± 8.9	151 ± 13	156
	30–50	22.4 ± 4.9	10.2 ± 3.7	7.4 ± 3.5	1.3 ± 1.0	2.1 ± 1.8	39.6 ± 6.2	82.9 ± 9.6	80
200–240	1–4	$0.11^{+0.33}_{-0.10}$	$0.37^{+0.72}_{-0.36}$	$0.7^{+1.1}_{-0.7}$	1.3 ± 1.0	$0.04^{+0.23}_{-0.03}$	3.0 ± 2.0	5.5 ± 2.5	2
	4–10	$0.75^{+0.90}_{-0.74}$	$0.15^{+0.50}_{-0.14}$	$1.4^{+1.5}_{-1.4}$	3.5 ± 1.7	$0.14^{+0.39}_{-0.13}$	11.9 ± 3.6	17.8 ± 4.4	19
	10–20	2.9 ± 1.7	7.9 ± 3.4	2.9 ± 2.2	2.5 ± 1.4	1.2 ± 1.2	42.8 ± 6.8	60.1 ± 8.3	59
	20–30	4.3 ± 2.1	4.7 ± 2.6	2.6 ± 2.0	1.1 ± 1.0	$0.27^{+0.54}_{-0.26}$	31.3 ± 5.8	44.3 ± 7.1	47
	30–50	5.7 ± 2.4	$0.6^{+1.0}_{-0.6}$	2.8 ± 2.1	$0.63^{+0.70}_{-0.62}$	$0.35^{+0.65}_{-0.34}$	17.6 ± 4.4	27.7 ± 5.6	24
240–290	1–4	< 0.02	< 0.1	$0.43^{+0.88}_{-0.42}$	0.8 ± 0.8	< 0.07	1.5 ± 1.3	2.7 ± 1.9	2
	4–10	$0.9^{+1.2}_{-0.9}$	$0.57^{+0.97}_{-0.56}$	$0.8^{+1.1}_{-0.8}$	1.5 ± 1.1	$0.3^{+2.6}_{-0.3}$	3.7 ± 2.0	7.7 ± 3.9	11
	10–20	2.4 ± 1.6	3.4 ± 2.3	1.6 ± 1.6	1.2 ± 0.9	$0.3^{+1.3}_{-0.3}$	14.9 ± 4.0	23.8 ± 5.4	19
	20–30	2.0 ± 1.5	2.4 ± 1.9	1.9 ± 1.7	$0.61^{+0.67}_{-0.60}$	$0.03^{+0.45}_{-0.02}$	10.1 ± 3.3	17.0 ± 4.5	13
	30–50	2.3 ± 1.7	$0.32^{+0.73}_{-0.31}$	$1.2^{+1.4}_{-1.1}$	$0.40^{+0.53}_{-0.39}$	$0.8^{+4.6}_{-0.7}$	6.6 ± 2.7	11.6 ± 5.8	10
> 290	1–4	< 0.02	< 0.1	$0.18^{+0.65}_{-0.17}$	$0.57^{+0.65}_{-0.56}$	< 0.01	$0.70^{+0.88}_{-0.69}$	1.5 ± 1.3	1
	4–10	$0.38^{+0.64}_{-0.37}$	$0.8^{+1.1}_{-0.8}$	$0.9^{+1.2}_{-0.9}$	1.3 ± 1.0	$0.12^{+0.44}_{-0.11}$	1.7 ± 1.3	5.2 ± 2.5	3
	10–20	1.3 ± 1.2	$0.8^{+1.2}_{-0.8}$	1.6 ± 1.6	1.05 ± 0.89	$0.9^{+1.4}_{-0.9}$	7.8 ± 2.9	13.5 ± 4.1	15
	20–30	$0.9^{+1.0}_{-0.9}$	$0.06^{+0.28}_{-0.05}$	$1.5^{+1.6}_{-1.5}$	$0.3^{+0.50}_{-0.34}$	< 0.09	5.9 ± 2.5	8.8 ± 3.2	13
	30–50	1.2 ± 1.1	< 0.1	$1.3^{+1.5}_{-1.3}$	$0.09^{+0.24}_{-0.08}$	$0.7^{+1.2}_{-0.7}$	3.6 ± 2.0	6.8 ± 3.0	9

Table 5: Observed and predicted yields as extracted from the maximum likelihood fit, in the 3ℓ-Ewk SRs. Uncertainties include both the statistical and systematic components.

p_T^{miss} [GeV]	$M_{SFOS}^{min}(\ell\ell)$ [GeV]	VV	WZ	Rare	Nonprompt	Total bkg	Data
	4–10	$0.18^{+0.54}_{-0.17}$	4.8 ± 1.9	$0.08^{+0.38}_{-0.07}$	$0.61^{+0.83}_{-0.60}$	5.7 ± 2.2	3
125–200	10–20	$0.08^{+0.35}_{-0.07}$	2.3 ± 1.3	$0.5^{+1.0}_{-0.5}$	1.9 ± 1.4	4.9 ± 2.2	7
	20–30	$0.03^{+0.23}_{-0.02}$	1.0 ± 1.0	$0.07^{+0.35}_{-0.06}$	1.3 ± 1.2	2.4 ± 1.5	4
	30–50	$0.01^{+0.13}_{-0.01}$	$0.39^{+0.55}_{-0.38}$	$0.08^{+0.37}_{-0.07}$	1.4 ± 1.2	1.8 ± 1.4	1
	1–4	$0.01^{+0.18}_{-0.01}$	1.5 ± 1.0	$0.03^{+0.20}_{-0.02}$	$0.18^{+0.44}_{-0.17}$	1.7 ± 1.2	3
	4–10	$0.05^{+0.34}_{-0.04}$	2.9 ± 1.4	$0.16^{+0.47}_{-0.15}$	$0.85^{+0.99}_{-0.84}$	4.0 ± 1.8	1
> 200	10–20	$0.06^{+0.32}_{-0.05}$	2.0 ± 1.2	$0.05^{+0.26}_{-0.04}$	2.1 ± 1.5	4.2 ± 2.0	5
	20–30	< 0.002	$0.52^{+0.60}_{-0.51}$	$0.06^{+0.29}_{-0.05}$	1.1 ± 1.1	1.7 ± 1.3	2
	30–50	< 0.002	$0.31^{+0.46}_{-0.30}$	$0.03^{+0.23}_{-0.02}$	1.0 ± 1.0	1.3 ± 1.1	1

Table 6: Observed and predicted yields as extracted from the maximum likelihood fit, in the WZ-like selection SRs. Uncertainties include both the statistical and systematic components.

p_T^{miss} [GeV]	$M_{SFOS}^{min}(\ell\ell)$ [GeV]	VV	WZ	Rare	Nonprompt	Total bkg	Data
	4–10	$0.13^{+0.47}_{-0.12}$	2.6 ± 1.4	$0.31^{+0.67}_{-0.30}$	$0.49^{+0.70}_{-0.48}$	3.5 ± 1.8	4
125–200	10–20	$0.14^{+0.47}_{-0.13}$	4.3 ± 1.8	$0.47^{+0.83}_{-0.46}$	1.2 ± 1.1	6.1 ± 2.3	11
	20–30	$0.17^{+0.51}_{-0.16}$	5.0 ± 2.0	$0.50^{+0.85}_{-0.49}$	2.1 ± 1.5	7.8 ± 2.6	9
	1–4	$0.16^{+0.56}_{-0.15}$	$0.11^{+0.29}_{-0.10}$	$0.06^{+0.33}_{-0.05}$	$0.44^{+0.66}_{-0.43}$	$0.78^{+0.97}_{-0.77}$	0
	4–10	$0.22^{+0.60}_{-0.21}$	2.6 ± 1.4	$0.10^{+0.38}_{-0.09}$	$0.24^{+0.59}_{-0.23}$	3.1 ± 1.6	3
> 200	10–20	$0.7^{+1.1}_{-0.7}$	10.6 ± 2.8	$0.9^{+1.1}_{-0.9}$	1.9 ± 1.4	14.0 ± 3.4	19
	20–30	$0.7^{+1.0}_{-0.7}$	15.2 ± 3.3	$1.2^{+1.3}_{-1.2}$	4.0 ± 2.0	21.0 ± 4.2	23

9 Interpretation

The results of the search are interpreted in the context of the SUSY scenarios described in Section 3. Limits on the production cross section for SUSY particle pairs as a function of their masses are computed using a modified frequentist approach that employs the CL_s criterion and an asymptotic formulation [85–88].

We express the results as upper limits at 95% confidence level (CL) on the potential presence of a SUSY signal in the data. The limits of the TCHIWZ simplified model for the production of a wino pair decaying into bino LSPs are shown for the two signal scenarios described in Section 3. When considering the full matrix element of the electroweakino decay, the relative sign of the eigenvalues of the neutralino mass matrix leads to two slightly different $M(\ell\ell)$ distributions in $\tilde{\chi}_2^0$ decays. The upper plot in Fig. 8 shows the limit for the scenario where the product of $\tilde{m}_{\tilde{\chi}_1^0}$, $\tilde{m}_{\tilde{\chi}_2^0}$ eigenvalues is positive, while the negative case is shown by the lower plot. The results are reweighted to account for the branching fraction modulation of the off-shell W and Z bosons, as mentioned in Section 3.

The observed exclusion limit shown in Fig. 8 is weaker than the expected one in the intermediate and high Δm ranges. This is due to data yields that are higher than the predictions in specific bins of the 2ℓ-Ewk SR (Table 4, ultra-MET bin, $20 < M(\ell\ell) \le 30$ GeV), the 3ℓ-Ewk SR

Table 7: Observed and predicted yields as extracted from the maximum likelihood fit, in the 2ℓ-Stop SRs. Uncertainties include both the statistical and systematic components.

p_T^{miss} [GeV]	$p_T(\ell_1)$ [GeV]	t$\bar{t}$	DY	VV	WZ	Rare	Nonprompt	Total bkg	Data
125–200	3.5–8	1.2 ± 1.2	5.2 ± 3.1	$1.0^{+1.2}_{-1.0}$	1.4 ± 1.1	$0.06^{+0.27}_{-0.05}$	41.0 ± 6.3	49.9 ± 7.2	52
	8–12	15.0 ± 4.0	22.9 ± 5.9	6.6 ± 3.1	6.0 ± 2.1	$0.96^{+0.99}_{-0.95}$	93.1 ± 9.4	144 ± 12	156
	12–16	31.8 ± 5.9	24.0 ± 6.1	13.7 ± 4.5	7.2 ± 2.4	2.8 ± 1.7	101.3 ± 9.9	180 ± 14	196
	16–20	59.9 ± 8.0	36.9 ± 7.5	19.8 ± 5.5	7.9 ± 2.5	4.2 ± 2.1	100.2 ± 9.8	229 ± 16	238
	20–25	103 ± 11	27.2 ± 6.5	33.2 ± 7.1	7.7 ± 2.5	7.5 ± 2.8	95.0 ± 9.5	273 ± 18	285
	25–30	114 ± 11	21.4 ± 5.7	35.5 ± 7.3	5.1 ± 2.0	8.0 ± 2.8	71.5 ± 8.3	256 ± 17	246
200–290	3.5–8	1.1 ± 1.0	1.7 ± 1.5	2.8 ± 2.1	2.9 ± 1.4	$0.04^{+0.20}_{-0.03}$	41.3 ± 6.6	49.9 ± 7.3	53
	8–12	11.0 ± 3.3	1.6 ± 1.5	7.3 ± 3.3	5.6 ± 2.0	$0.43^{+0.65}_{-0.42}$	103 ± 10	129 ± 12	130
	12–16	24.1 ± 4.9	5.0 ± 2.6	17.1 ± 5.0	5.5 ± 2.0	2.9 ± 1.7	102 ± 10	156 ± 13	153
	16–20	40.3 ± 6.3	11.7 ± 4.2	24.7 ± 6.1	5.6 ± 2.0	2.4 ± 1.6	92.0 ± 9.8	177 ± 14	163
	20–25	69.9 ± 8.3	7.6 ± 3.4	41.9 ± 7.9	6.7 ± 2.2	5.0 ± 2.2	89.3 ± 9.7	220 ± 16	220
	25–30	69.0 ± 8.3	11.8 ± 4.1	47.3 ± 8.4	5.9 ± 2.0	9.6 ± 3.1	74.2 ± 8.9	218 ± 16	219
290–340	3.5–8	$0.15^{+0.35}_{-0.14}$	$0.67^{+0.90}_{-0.66}$	$0.34^{+0.72}_{-0.33}$	$0.29^{+0.44}_{-0.28}$	< 0.05	2.7 ± 1.7	4.1 ± 2.1	4
	8–12	1.9 ± 1.4	$0.8^{+1.1}_{-0.8}$	1.9 ± 1.7	$0.64^{+0.67}_{-0.63}$	$0.01^{+0.11}_{-0.01}$	9.9 ± 3.2	15.0 ± 4.1	15
	12–16	3.4 ± 1.8	$0.33^{+0.61}_{-0.32}$	3.4 ± 2.3	0.69 ± 0.69	$0.64^{+0.85}_{-0.63}$	6.4 ± 2.6	14.8 ± 4.1	16
	16–20	5.5 ± 2.3	$0.8^{+1.1}_{-0.8}$	4.5 ± 2.6	0.91 ± 0.80	1.0 ± 1.0	11.8 ± 3.5	24.6 ± 5.2	23
	20–25	8.1 ± 2.8	$0.9^{+1.2}_{-0.9}$	7.6 ± 3.4	1.24 ± 0.93	$0.82^{+0.89}_{-0.81}$	10.1 ± 3.2	28.8 ± 5.8	30
	25–30	8.8 ± 2.9	$0.58^{+0.97}_{-0.57}$	8.6 ± 3.6	0.96 ± 0.81	1.7 ± 1.3	10.8 ± 3.4	31.5 ± 6.0	38
> 340	3.5–8	$0.12^{+0.37}_{-0.11}$	$0.14^{+0.51}_{-0.13}$	$0.48^{+0.86}_{-0.47}$	$0.29^{+0.46}_{-0.28}$	< 0.03	3.7 ± 2.0	4.7 ± 2.3	7
	8–12	1.8 ± 1.3	$0.22^{+0.59}_{-0.21}$	1.5 ± 1.5	0.78 ± 0.75	$0.02^{+0.12}_{-0.01}$	7.8 ± 2.9	12.2 ± 3.6	11
	12–16	2.4 ± 1.5	$0.31^{+0.63}_{-0.30}$	3.5 ± 2.3	0.87 ± 0.78	$0.60^{+0.79}_{-0.59}$	4.0 ± 2.0	11.6 ± 3.6	14
	16–20	4.0 ± 2.0	$0.64^{+0.89}_{-0.63}$	4.9 ± 2.7	0.80 ± 0.75	$0.90^{+0.93}_{-0.89}$	5.5 ± 2.5	16.7 ± 4.4	11
	20–25	5.8 ± 2.3	$0.62^{+0.95}_{-0.61}$	8.6 ± 3.6	1.22 ± 0.93	$0.84^{+0.92}_{-0.83}$	8.6 ± 3.0	25.7 ± 5.5	26
	25–30	6.5 ± 2.5	$0.7^{+1.0}_{-0.7}$	9.3 ± 3.7	1.12 ± 0.88	2.6 ± 1.6	7.7 ± 2.9	27.9 ± 5.7	25
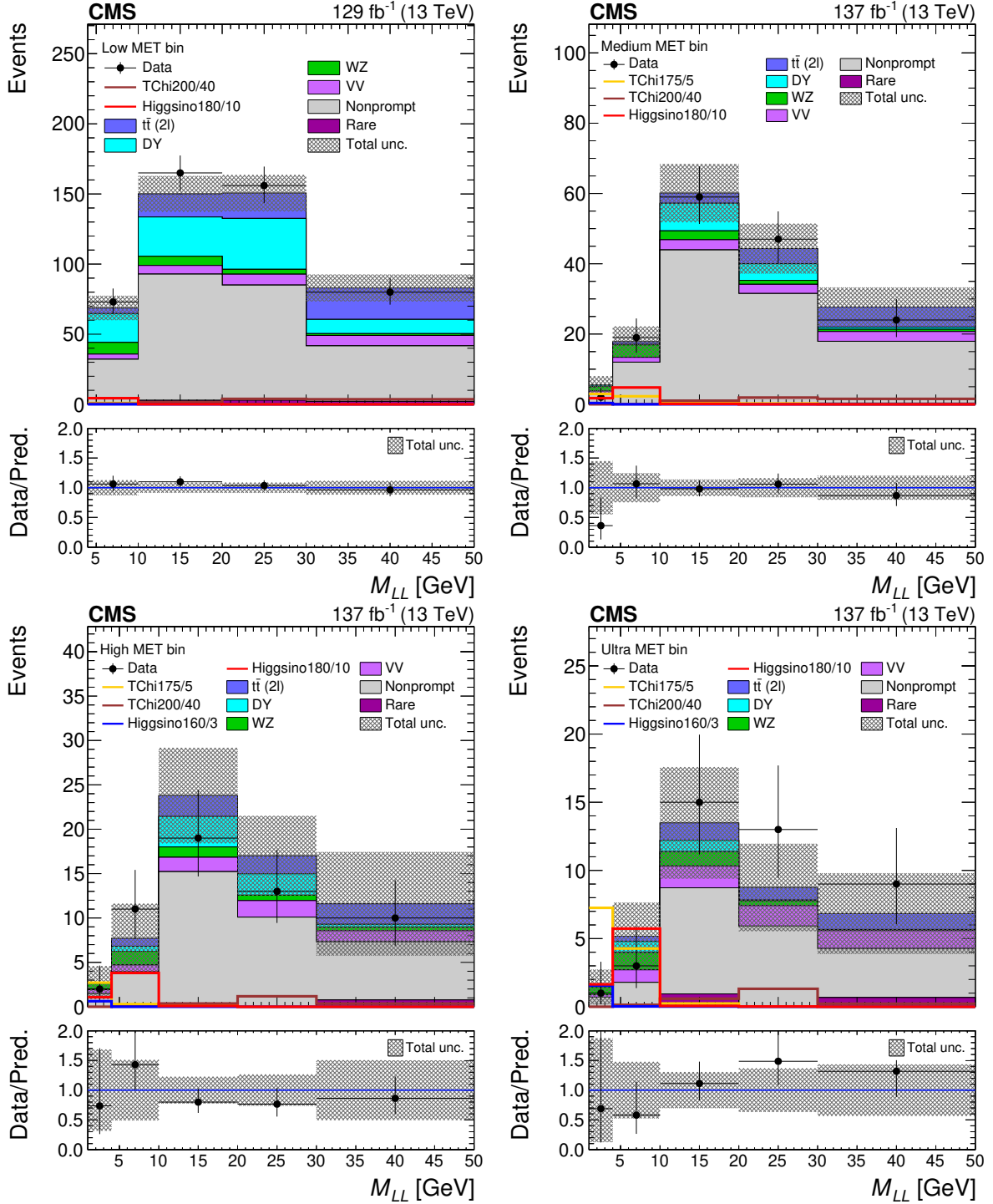
Figure 5: The 2ℓ-Ewk SR: the post-fit distribution of the $M(\ell\ell)$ variable is shown for the low- (upper left), medium- (upper right), high- (lower left) and ultra- (lower right) MET bins. Uncertainties include both the statistical and systematic components. The signal distributions overlaid on the plot are from the TCHIWZ and the simplified higgsino models in the scenario where the product of $\widetilde{m}_{\widetilde{\chi}_1^0}\widetilde{m}_{\widetilde{\chi}_2^0}$ eigenvalues is positive and negative, respectively. The numbers after the model name in the legend indicate the mass of the NLSP and the mass splitting between the NLSP and LSP, in GeV.
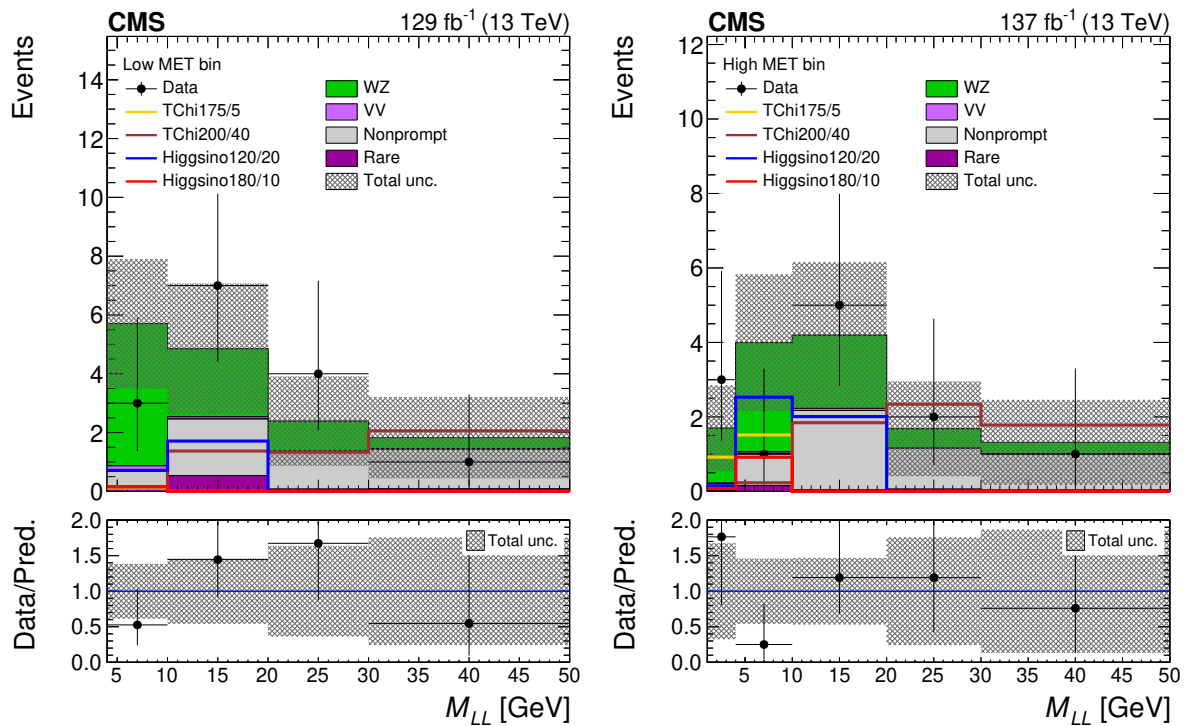
Figure 6: The 3ℓ-Ewk search regions: the post-fit distribution of the $M_{\mathrm{SFOS}}^{\min}(\ell\ell)$ variable is shown for the low- (left) and high- (right) MET bins. Uncertainties include both the statistical and systematic components. The signal distributions overlaid on the plot are from the TCHIWZ and the simplified higgsino models in the scenario where the product of $\widetilde{m}_{\widetilde{\chi}_1^0}\widetilde{m}_{\widetilde{\chi}_2^0}$ eigenvalues is positive and negative, respectively. The numbers after the model name in the legend indicate the mass of the NLSP and the mass splitting between the NLSP and LSP, in GeV.
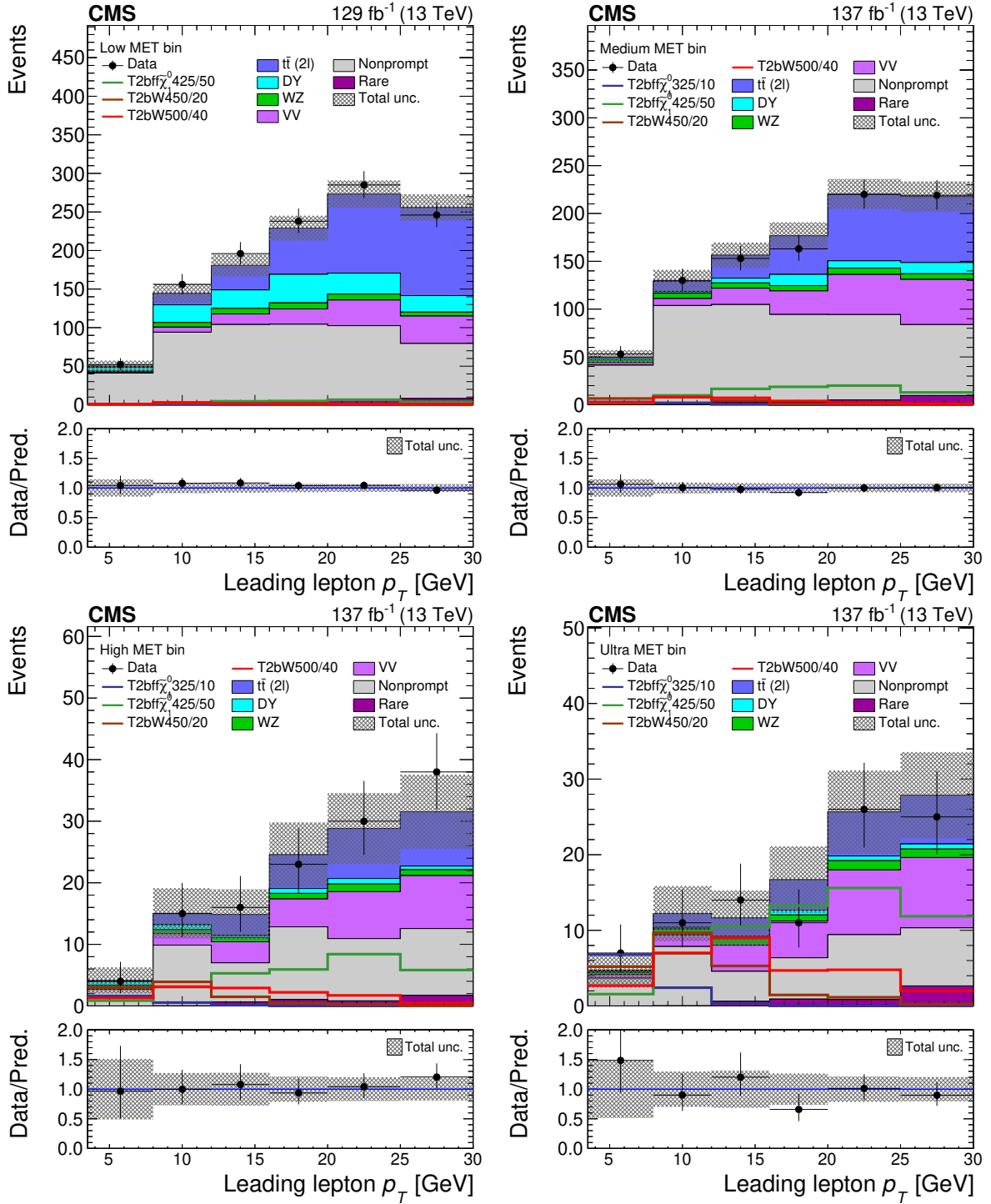
Figure 7: The 2ℓ-Stop SR: the post-fit distribution of the leading lepton p_T variable is shown for the low- (upper left), medium- (upper right), high- (lower left) and ultra- (lower right) MET bins. Uncertainties include both the statistical and systematic components. The signal distributions overlaid on the plot are from the T2Bff$\widetilde{\chi}_1^0$ and the T2BW models. The numbers after the model name in the legend indicate the mass of the top squark and the mass splitting between the top squark and LSP, in GeV.

(Table 5, low-MET bin, $10 < M_{\text{SFOS}}^{\min}(\ell\ell) \leq 30\,\text{GeV}$) and WZ-like selection SR (Table 6, low- and high-MET bin, $10 < M_{\text{SFOS}}^{\min}(\ell\ell) \leq 20\,\text{GeV}$). The shift of the $M(\ell\ell)$ distribution for the negative case for the product of $\widetilde{m}_{\widetilde{\chi}_1^0}$, $\widetilde{m}_{\widetilde{\chi}_2^0}$ eigenvalues causes the observed upper limit signal cross section to be higher, leading to a smaller range of excluded mass parameters in this scenario. The excess has a maximum local significance of 2.4 standard deviations for the signal mass point with $m_{\widetilde{\chi}_2^0} = 125\,\text{GeV}$ and $\Delta m = 40\,\text{GeV}$.

The upper plot of Fig. 9 displays the space of allowed electroweakino masses for the higgsino simplified model, assuming a chargino with mass halfway between the two lightest neutralinos. The simplified higgsino model includes neutralino pair production and neutralino-chargino production, while the pMSSM higgsino model includes all possible production modes. The dilepton invariant mass distributions are reweighted for the case where $\widetilde{m}_{\widetilde{\chi}_1^0}\widetilde{m}_{\widetilde{\chi}_2^0} < 0$, since this is the combination allowed when the higgsino is the LSP. The results also take into account the off-shell W and Z boson branching fraction corrections mentioned in Section 3. A weaker than expected observed exclusion limit in the higher Δm region is present also for this interpretation for the reasons mentioned above.

The expected and observed exclusion contours for the pMSSM higgsino model are shown in the lower plot of Fig. 9. The limits are presented in the plane of the higgsino-bino mass parameters μ-M_1. In the pMSSM, larger μ values roughly correspond to larger masses for the parent SUSY particles. Larger values of the M_1 parameter correspond to smaller values of the mass difference between the LSP and its parent SUSY particle. Due to this, the fact that the observed limit is weaker than the expected one for intermediate and higher Δm values of the TChiWZ and higgsino simplified models manifests at small M_1 values for the pMSSM higgsino model.

For direct production of top squarks, the 2ℓ-Stop SRs are instead used in the maximum likelihood fit to extract upper limits on the T2bff$\widetilde{\chi}_1^0$ and T2bW models presented in Section 3. Figure 10 shows the limits of the T2bff$\widetilde{\chi}_1^0$ (upper) and T2bW (lower) simplified models. For both models, the corrections for the modulation of the off-shell W bosons branching fraction are considered. The drop in the exclusion line around $\Delta m = 20\,\text{GeV}$ is caused by the smaller acceptance when going to lower Δm, which is due to the minimum lepton p_{T} requirements of the SRs.
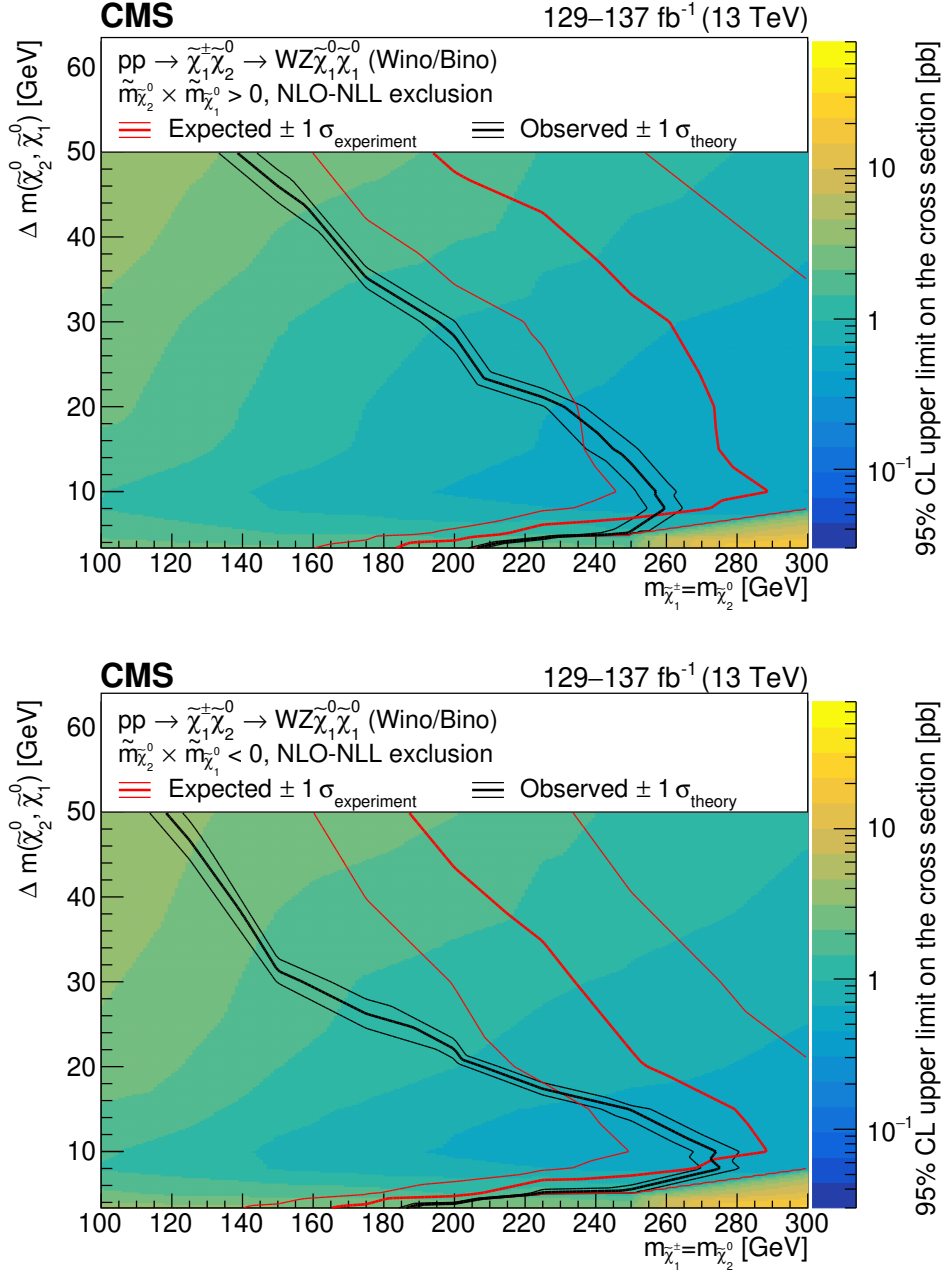
Figure 8: The observed 95% CL exclusion contours (black curves) assuming the NLO+NLL cross sections, with the variations (thin lines) corresponding to the uncertainty in the cross section for the TCHIWZ model. The red curves present the 95% CL expected limits with the band (thin lines) covering 68% of the limits in the absence of signal. Results are reported for the $\widetilde{m}_{\widetilde{\chi}_2^0}\widetilde{m}_{\widetilde{\chi}_1^0} > 0(< 0)$ $M(\ell\ell)$ spectrum reweighting scenario in the upper (lower) plot. The range of luminosities of the analysis regions included in the fit is indicated on the plot.
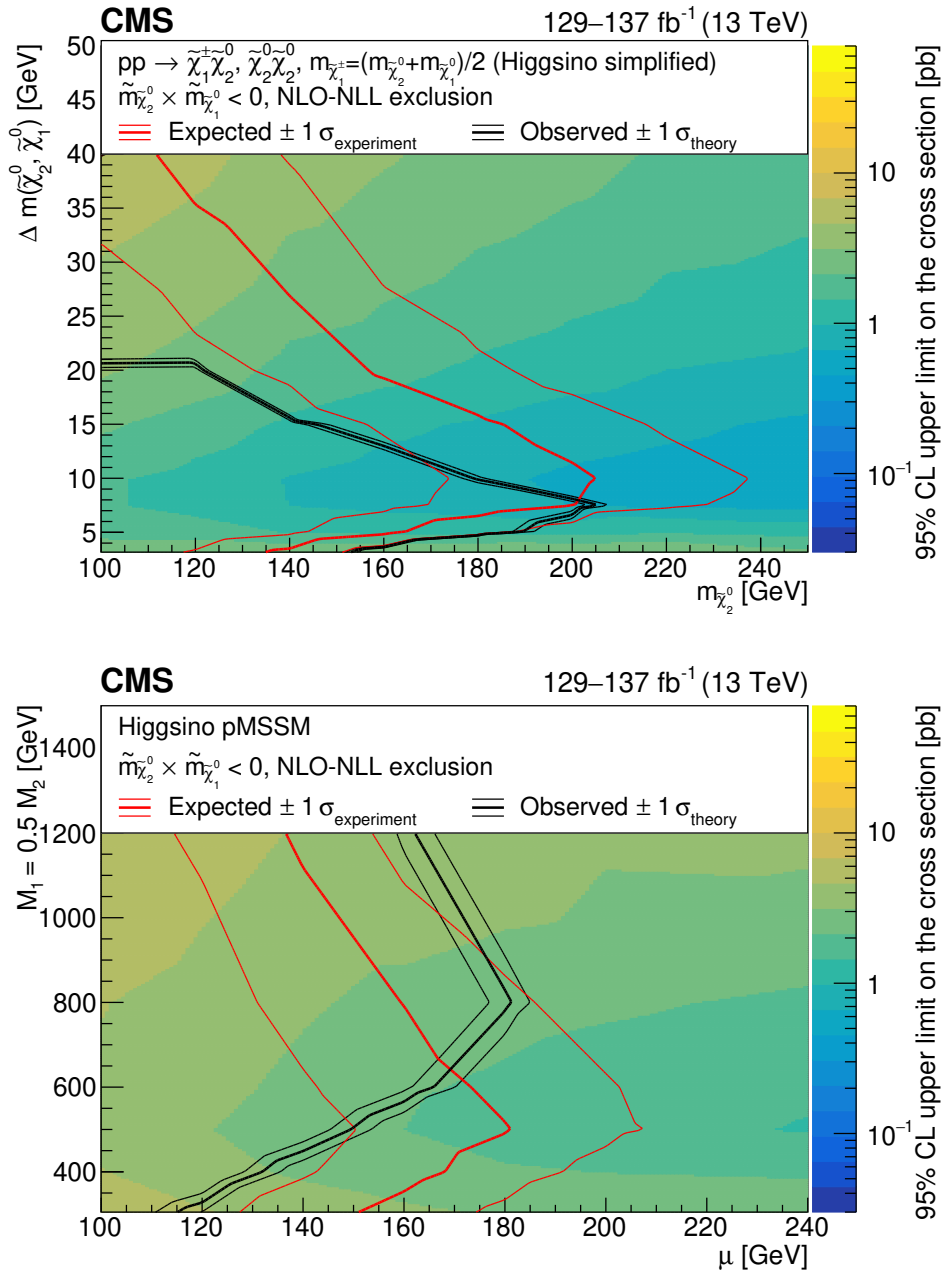
Figure 9: The observed 95% CL exclusion contours (black curves) assuming the NLO+NLL cross sections, with the variations (thin lines) corresponding to the uncertainty in the cross section for the simplified (upper) and the pMSSM (lower) higgsino models. The simplified model includes both neutralino pair and neutralino-chargino production modes, while the pMSSM one includes all possible production modes. The red curves present the 95% CL expected limits with the band (thin lines) covering 68% of the limits in the absence of signal. The results are reported for the $\widetilde{m}_{\tilde{\chi}_2^0} \widetilde{m}_{\tilde{\chi}_1^0} < 0$ $M(\ell\ell)$ spectrum reweighting scenario. The range of luminosities of the analysis regions included in the fit is indicated on the plot.
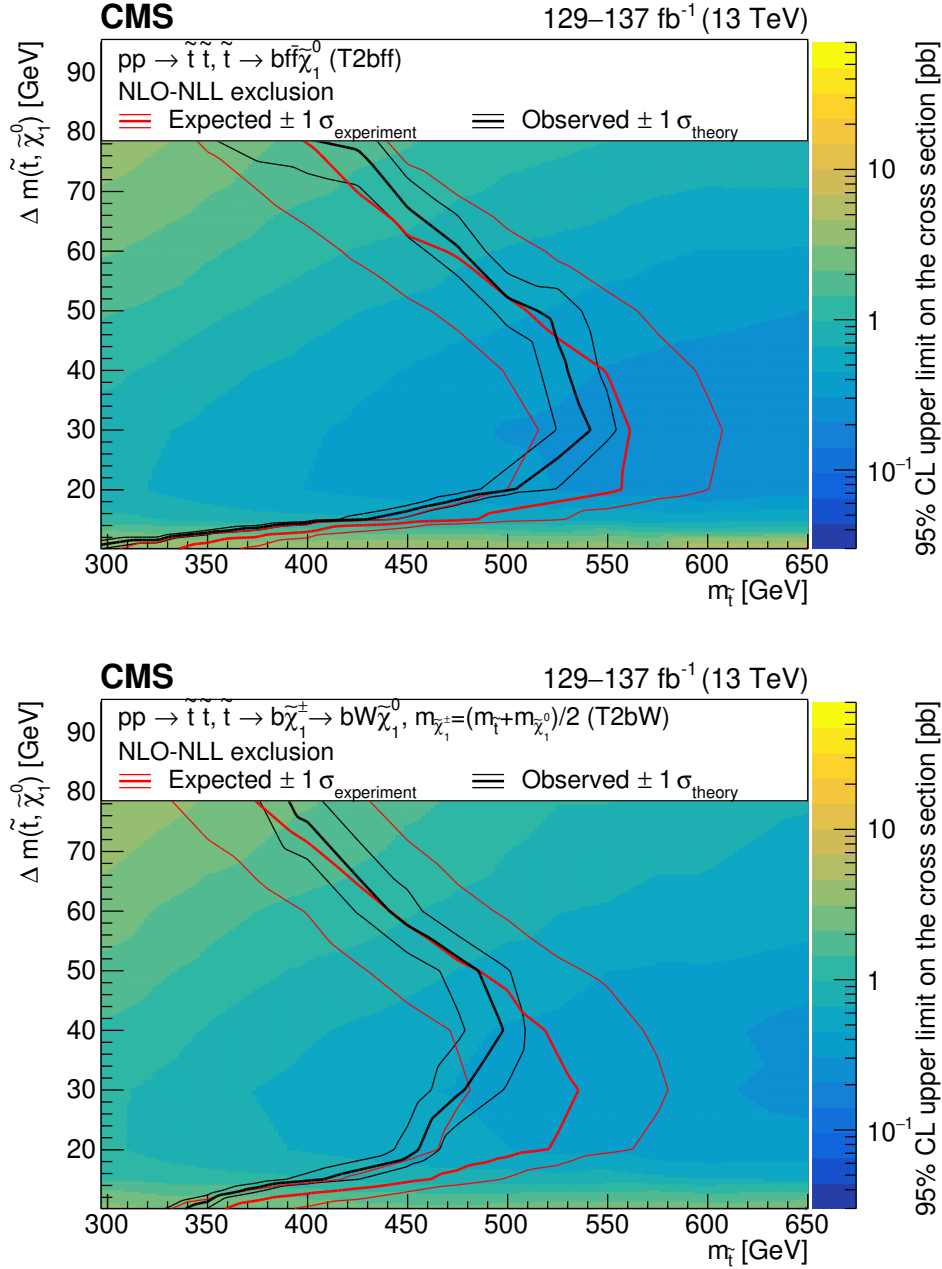
Figure 10: The observed 95% CL exclusion contours (black curves) assuming the NLO+NLL cross sections, with the variations (thin lines) corresponding to the uncertainty in the cross section for the T2Bff$\widetilde{\chi}_1^0$ (upper) and T2BW (lower) simplified models. The red curves present the 95% CL expected limits with the band (thin lines) covering 68% of the limits in the absence of signal. The range of luminosities of the analysis regions included in the fit is indicated on the plot.

10 Summary

A search for new physics is performed using events with two or three soft leptons and missing transverse momentum. These signatures are motivated by models predicting a weakly interacting massive particle that originates from the decay of another new particle with nearly degenerate mass. The results are based on data collected by the CMS experiment at the LHC during 2016–2018, corresponding to an integrated luminosity of up to $137\,\text{fb}^{-1}$. The observed event yields are in agreement with the standard model expectations.

The results are interpreted in the framework of supersymmetric (SUSY) simplified models targeting electroweakino mass-degenerate spectra and top squark-lightest neutralino $(\tilde{t}\text{-}\tilde{\chi}_1^0)$ mass-degenerate benchmark models. An interpretation of the analysis is performed also in the phenomenological minimal SUSY standard model (pMSSM) framework. In particular, the simplified wino-bino model in which the next-to-lightest neutralino and the lightest chargino are produced and decay according to $\tilde{\chi}_2^0 \tilde{\chi}_1^{\pm} \to Z^* W^* \tilde{\chi}_1^0 \tilde{\chi}_1^0$ are explored for mass differences (Δm) between $\tilde{\chi}_2^0$ and $\tilde{\chi}_1^0$ of less than $50\,\text{GeV}$, assuming wino production cross sections. At 95% confidence level, wino-like $\tilde{\chi}_1^{\pm}/\tilde{\chi}_2^0$ masses are excluded up to $275\,\text{GeV}$ for Δm of $10\,\text{GeV}$ relative to the lightest neutralino. The higgsino simplified model is of particular interest; mass-degenerate electroweakinos are expected in natural SUSY, which predicts light higgsinos. In this model, excluded masses reach up to $205\,\text{GeV}$ for Δm of $7.5\,\text{GeV}$ and $150\,\text{GeV}$ for a highly compressed scenario with Δm of $3\,\text{GeV}$. In the pMSSM higgsino model, the limits are presented in the plane of the higgsino-bino mass parameters μ-M_1; the higgsino mass parameter μ is excluded up to $170\,\text{GeV}$, when the bino mass parameter M_1 is $600\,\text{GeV}$. For larger values of M_1, the mass splitting $\Delta m(\tilde{\chi}_2^0, \tilde{\chi}_1^0)$ becomes smaller; for $M_1 = 800\,\text{GeV}$, μ is excluded up to $180\,\text{GeV}$. Finally, two $\tilde{t}\text{-}\tilde{\chi}_1^0$ mass-degenerate benchmark models are considered. Top squarks with masses below 540 (480) GeV are excluded for the four-body (chargino-mediated) top squark decay model, with a $(\tilde{t}\text{-}\tilde{\chi}_1^0)$ mass splitting at $30\,\text{GeV}$.

References

[1] J. Wess and B. Zumino, "Supergauge transformations in four dimensions", *Nucl. Phys. B* **70** (1974) 39, `doi:10.1016/0550-3213(74)90355-1`.

[2] H. P. Nilles, "Supersymmetry, supergravity and particle physics", *Phys. Rept.* **110** (1984) 1, `doi:10.1016/0370-1573(84)90008-5`.

[3] H. E. Haber and G. L. Kane, "The search for supersymmetry: Probing physics beyond the standard model", *Phys. Rept.* **117** (1985) 75, `doi:10.1016/0370-1573(85)90051-1`.

[4] R. Barbieri, S. Ferrara, and C. A. Savoy, "Gauge models with spontaneously broken local supersymmetry", *Phys. Lett. B* **119** (1982) 343, `doi:10.1016/0370-2693(82)90685-2`.

[5] S. Dawson, E. Eichten, and C. Quigg, "Search for supersymmetric particles in hadron-hadron collisions", *Phys. Rev. D* **31** (1985) 1581, `doi:10.1103/PhysRevD.31.1581`.

[6] R. Barbieri and G. Giudice, "Upper bounds on supersymmetric particle masses", *Nucl. Phys. B* **306** (1988) 63, `doi:10.1016/0550-3213(88)90171-X`.

[7] E. Witten, "Dynamical breaking of supersymmetry", *Nucl. Phys. B* **188** (1981) 513, `doi:10.1016/0550-3213(81)90006-7`.

[8] S. Dimopoulos and H. Georgi, "Softly broken supersymmetry and SU(5)", *Nucl. Phys. B* **193** (1981) 150, `doi:10.1016/0550-3213(81)90522-8`.

[9] G. R. Farrar and P. Fayet, "Phenomenology of the production, decay, and detection of new hadronic states associated with supersymmetry", *Phys. Lett. B* **76** (1978) 575, `doi:10.1016/0370-2693(78)90858-4`.

[10] Particle Data Group, P. A. Zyla et al., "Review of particle physics", *Prog. Theor. Exp. Phys.* **2020** (2020) 083C01, `doi:10.1093/ptep/ptaa104`.

[11] B. de Carlos and J. Casas, "One-loop analysis of the electroweak breaking in supersymmetric models and the fine-tuning problem", *Phys. Lett. B* **309** (1993) 320, `doi:10.1016/0370-2693(93)90940-J`, `arXiv:hep-ph/9303291`.

[12] M. Dine, W. Fischler, and M. Srednicki, "Supersymmetric technicolor", *Nucl. Phys. B* **189** (1981) 575, `doi:10.1016/0550-3213(81)90582-4`.

[13] S. Dimopoulos and S. Raby, "Supercolor", *Nucl. Phys. B* **192** (1981) 353, `doi:10.1016/0550-3213(81)90430-2`.

[14] N. Sakai, "Naturalness in supersymmetric GUTS", *Z. Phys. C* **11** (1981) 153, `doi:10.1007/BF01573998`.

[15] R. K. Kaul and P. Majumdar, "Cancellation of quadratically divergent mass corrections in globally supersymmetric spontaneously broken gauge theories", *Nucl. Phys. B* **199** (1982) 36, `doi:10.1016/0550-3213(82)90565-X`.

[16] K. Griest and D. Seckel, "Three exceptions in the calculation of relic abundances", *Phys. Rev. D* **43** (1991) 3191, `doi:10.1103/PhysRevD.43.3191`.

[17] J. Edsjo and P. Gondolo, "Neutralino relic density including coannihilations", *Phys. Rev. D* **56** (1997) 1879, `doi:10.1103/PhysRevD.56.1879`, `arXiv:hep-ph/9704361`.

[18] H. Baer, V. Barger, and P. Huang, "Hidden SUSY at the LHC: the light higgsino-world scenario and the role of a lepton collider", *JHEP* **11** (2011) 031, `doi:10.1007/JHEP11(2011)031`, `arXiv:1107.5581`.

[19] H. Baer, A. Mustafayev, and X. Tata, "Monojet plus soft dilepton signal from light higgsino pair production at LHC14", *Phys. Rev. D* **90** (2014) 115007, `doi:10.1103/PhysRevD.90.115007`, `arXiv:1409.7058`.

[20] C. Han et al., "Probing light higgsinos in natural SUSY from monojet signals at the LHC", *JHEP* **02** (2014) 049, `doi:10.1007/JHEP02(2014)049`, `arXiv:1310.4274`.

[21] Z. Han, G. D. Kribs, A. Martin, and A. Menon, "Hunting quasidegenerate higgsinos", *Phys. Rev. D* **89** (2014) 075007, `doi:10.1103/PhysRevD.89.075007`, `arXiv:1401.1235`.

[22] MSSM Working Group, "The minimal supersymmetric standard model: Group summary report", 1998. `arXiv:hep-ph/9901246`.

[23] C. Balázs, M. Carena, and C. E. M. Wagner, "Dark matter, light stops and electroweak baryogenesis", *Phys. Rev. D* **70** (2004) 015007, `doi:10.1103/PhysRevD.70.015007`, `arXiv:hep-ph/0403224`.

[24] CMS Collaboration, "Search for supersymmetry in events with soft leptons, low jet multiplicity, and missing transverse energy in proton–proton collisions at $\sqrt{s} = 8\,\text{TeV}$", *Phys. Lett. B* **759** (2016) 9, `doi:10.1016/j.physletb.2016.05.033`, `arXiv:1512.08002`.

[25] CMS Collaboration, "Search for new physics in events with two soft oppositely charged leptons and missing transverse momentum in proton–proton collisions at $\sqrt{s} = 13\,\text{TeV}$", *Phys. Lett. B* **782** (2018) 440, `doi:10.1016/j.physletb.2018.05.062`, `arXiv:1801.01846`.

[26] ATLAS Collaboration, "Search for electroweak production of supersymmetric states in scenarios with compressed mass spectra at $\sqrt{s} = 13\,\text{TeV}$ with the ATLAS detector", *Phys. Rev. D* **97** (2018) 052010, `doi:10.1103/PhysRevD.97.052010`, `arXiv:1712.08119`.

[27] ATLAS Collaboration, "Searches for electroweak production of supersymmetric particles with compressed mass spectra in $\sqrt{s} = 13\,\text{TeV}$ pp collisions with the ATLAS detector", *Phys. Rev. D* **101** (2020) 052005, `doi:10.1103/PhysRevD.101.052005`, `arXiv:1911.12606`.

[28] ATLAS Collaboration, "Search for chargino-neutralino pair production in final states with three leptons and missing transverse momentum in $\sqrt{s} = 13\,\text{TeV}$ pp collisions with the ATLAS detector", 2021. `arXiv:2106.01676`. Submitted to *Eur. Phys. J. C*.

[29] "HEPData record for this analysis", 2021. `doi:10.17182/hepdata.114415`.

[30] CMS Collaboration, "Performance of the CMS level-1 trigger in proton-proton collisions at $\sqrt{s} = 13\,\text{TeV}$", *JINST* **15** (2020) P10017, `doi:10.1088/1748-0221/15/10/P10017`, `arXiv:2006.10165`.

[31] CMS Collaboration, "The CMS trigger system", *JINST* **12** (2017) P01020, `doi:10.1088/1748-0221/12/01/P01020`, `arXiv:1609.02366`.

[32] CMS Collaboration, "The CMS experiment at the CERN LHC", *JINST* **3** (2008) P08004, `doi:10.1088/1748-0221/3/08/S08004`.

[33] J. Alwall et al., "The automated computation of tree-level and next-to-leading order differential cross sections, and their matching to parton shower simulations", *JHEP* **07** (2014) 079, `doi:10.1007/JHEP07(2014)079`, `arXiv:1405.0301`.

[34] R. Frederix and S. Frixione, "Merging meets matching in MC@NLO", *JHEP* **12** (2012) 061, `doi:10.1007/JHEP12(2012)061`, `arXiv:1209.6215`.

[35] J. Alwall et al., "Comparative study of various algorithms for the merging of parton showers and matrix elements in hadronic collisions", *Eur. Phys. J. C* **53** (2008) 473, `doi:10.1140/epjc/s10052-007-0490-5`, `arXiv:0706.2569`.

[36] P. Nason, "A new method for combining NLO QCD with shower Monte Carlo algorithms", *JHEP* **11** (2004) 040, `doi:10.1088/1126-6708/2004/11/040`, `arXiv:hep-ph/0409146`.

[37] S. Frixione, P. Nason, and C. Oleari, "Matching NLO QCD computations with parton shower simulations: the POWHEG method", *JHEP* **11** (2007) 070, `doi:10.1088/1126-6708/2007/11/070`, `arXiv:0709.2092`.

[38] S. Alioli, P. Nason, C. Oleari, and E. Re, "A general framework for implementing NLO calculations in shower Monte Carlo programs: the POWHEG BOX", *JHEP* **06** (2010) 043, `doi:10.1007/JHEP06(2010)043`, `arXiv:1002.2581`.

[39] T. Melia, P. Nason, R. Röntsch, and G. Zanderighi, "W^+W^-, WZ and ZZ production in the POWHEG BOX", *JHEP* **11** (2011) 078, `doi:10.1007/JHEP11(2011)078`, `arXiv:1107.5051`.

[40] P. Nason and G. Zanderighi, "W^+W^-, WZ and ZZ production in the POWHEG-BOX-V2", *Eur. Phys. J. C* **74** (2014) 2702, `doi:10.1140/epjc/s10052-013-2702-5`, `arXiv:1311.1365`.

[41] E. Re, "Single-top Wt-channel production matched with parton showers using the POWHEG method", *Eur. Phys. J. C* **71** (2011) 1547, `doi:10.1140/epjc/s10052-011-1547-z`, `arXiv:1009.2450`.

[42] NNPDF Collaboration, "Parton distributions for the LHC Run II", *JHEP* **04** (2015) 040, `doi:10.1007/JHEP04(2015)040`, `arXiv:1410.8849`.

[43] NNPDF Collaboration, "Parton distributions from high-precision collider data", *Eur. Phys. J. C* **77** (2017) 663, `doi:10.1140/epjc/s10052-017-5199-5`.

[44] T. Sjöstrand et al., "An introduction to PYTHIA 8.2", *Comput. Phys. Commun.* **191** (2015) 159, `doi:10.1016/j.cpc.2015.01.024`, `arXiv:1410.3012`.

[45] P. Skands, S. Carrazza, and J. Rojo, "Tuning PYTHIA 8.1: the Monash 2013 tune", *Eur. Phys. J. C* **74** (2014) 3024, `doi:10.1140/epjc/s10052-014-3024-y`, `arXiv:1404.5630`.

[46] CMS Collaboration, "Event generator tunes obtained from underlying event and multiparton scattering measurements", *Eur. Phys. J. C* **76** (2016) 155, `doi:10.1140/epjc/s10052-016-3988-x`, `arXiv:1512.00815`.

[47] CMS Collaboration, "Extraction and validation of a new set of CMS PYTHIA8 tunes from underlying-event measurements", *Eur. Phys. J. C* **80** (2020) 7499, `doi:10.1140/epjc/s10052-019-7499-4`, `arXiv:1903.12179`.

[48] GEANT4 Collaboration, "GEANT4—a simulation toolkit", *Nucl. Instrum. Meth. A* **506** (2003) 250, `doi:10.1016/S0168-9002(03)01368-8`.

[49] J. Alwall, P. Schuster, and N. Toro, "Simplified models for a first characterization of new physics at the LHC", *Phys. Rev. D* **79** (2009) 075020, `doi:10.1103/PhysRevD.79.075020`, `arXiv:0810.3921`.

[50] D. Alves et al., "Simplified models for LHC new physics searches", *J. Phys. G* **39** (2012) 105005, `doi:10.1088/0954-3899/39/10/105005`, `arXiv:1105.2838`.

[51] CMS Collaboration, "Interpretation of searches for supersymmetry with simplified models", *Phys. Rev. D* **88** (2013) 052017, `doi:10.1103/PhysRevD.88.052017`, `arXiv:1301.2175`.

[52] W. Beenakker et al., "Production of charginos, neutralinos, and sleptons at hadron colliders", *Phys. Rev. Lett.* **83** (1999) 3780, `doi:10.1103/PhysRevLett.83.3780`, `arXiv:hep-ph/9906298`. [Erratum: `doi:10.1103/PhysRevLett.100.029901`].

[53] B. Fuks, M. Klasen, D. R. Lamprea, and M. Rothering, "Gaugino production in proton-proton collisions at a center-of-mass energy of 8 TeV", *JHEP* **10** (2012) 081, `doi:10.1007/JHEP10(2012)081`, `arXiv:1207.2159`.

[54] B. Fuks, M. Klasen, D. R. Lamprea, and M. Rothering, "Precision predictions for electroweak superpartner production at hadron colliders with RESUMMINO", *Eur. Phys. J. C* **73** (2013) 2480, `doi:10.1140/epjc/s10052-013-2480-0`, `arXiv:1304.0790`.

[55] W. Beenakker, R. Hopker, and M. Spira, "PROSPINO: A program for the production of supersymmetric particles in next-to-leading order QCD", 1996. `arXiv:hep-ph/9611232`.

[56] A. Djouadi, J.-L. Kneur, and G. Moultaka, "SuSpect: A Fortran code for the supersymmetric and higgs particle spectrum in the MSSM", *Comput. Phys. Commun.* **176** (2007) 426, `doi:10.1016/j.cpc.2006.11.009`, `arXiv:hep-ph/0211331`.

[57] M. Mühlleitner, A. Djouadi, and Y. Mambrini, "SDECAY: A Fortran code for the decays of the supersymmetric particles in the MSSM", *Comput. Phys. Commun.* **168** (2005) 46, `doi:10.1016/j.cpc.2005.01.012`, `arXiv:hep-ph/0311167`.

[58] A. Djouadi, J. Kalinowski, and M. Spira, "HDECAY: A program for Higgs boson decays in the standard model and its supersymmetric extension", *Comput. Phys. Commun.* **108** (1998) 56, `doi:10.1016/S0010-4655(97)00123-9`, `arXiv:hep-ph/9704448`.

[59] M. M. Mühlleitner, A. Djouadi, and M. Spira, "Decays of supersymmetric particles: The program SUSY-HIT", in *Physics at LHC. Proc. 3rd Conf.*, p. 635. 2006. `arXiv:hep-ph/0609292`. *Acta Phys. Polon. B* **38** (2007) 635.

[60] P. Z. Skands et al., "SUSY Les Houches accord: Interfacing SUSY spectrum calculators, decay packages, and event generators", *JHEP* **07** (2004) 036, `doi:10.1088/1126-6708/2004/07/036`, `arXiv:hep-ph/0311123`.

[61] U. De Sanctis, T. Lari, S. Montesano, and C. Troncon, "Perspectives for the detection and measurement of supersymmetry in the focus point region of mSUGRA models with the ATLAS detector at LHC", *Eur. Phys. J. C* **52** (2007) 743, `doi:10.1140/epjc/s10052-007-0415-3`, `arXiv:0704.2515`.

[62] R. Gröber, M. M. Mühlleitner, E. Popenda, and A. Wlotzka, "Light stop decays: Implications for LHC searches", *Eur. Phys. J. C* **75** (2015) 420, `doi:10.1140/epjc/s10052-015-3626-z`, `arXiv:1408.4662`.

[63] CMS Collaboration, "The fast simulation of the CMS detector at LHC", *J. Phys. Conf. Ser.* **331** (2011) 032049, `doi:10.1088/1742-6596/331/3/032049`.

[64] A. Giammanco, "The fast simulation of the CMS experiment", *J. Phys. Conf. Ser.* **513** (2014) 022012, `doi:10.1088/1742-6596/513/2/022012`.

[65] CMS Collaboration, "Identification of heavy-flavour jets with the CMS detector in pp collisions at 13 TeV", *JINST* **13** (2018) P5011, `doi:10.1088/1748-0221/13/05/P05011`, `arXiv:1712.07158`.

[66] E. Chabanat and N. Estre, "Deterministic annealing for vertex finding at CMS", in *Proceedings of Computing in High Energy Physics and Nuclear Physics 2004*, p. 287. 2005. `doi:10.5170/CERN-2005-002.287`.

[67] M. Cacciari, G. P. Salam, and G. Soyez, "The anti-k_T jet clustering algorithm", *JHEP* **04** (2008) 063, `doi:10.1088/1126-6708/2008/04/063`, `arXiv:0802.1189`.

[68] M. Cacciari, G. P. Salam, and G. Soyez, "FastJet user manual", *Eur. Phys. J. C* **72** (2012) 1896, `doi:10.1140/epjc/s10052-012-1896-2`, `arXiv:1111.6097`.

[69] CMS Collaboration, "Pileup mitigation at CMS in 13 TeV data", *JINST* **15** (2020) P09018, `doi:10.1088/1748-0221/15/09/p09018`, `arXiv:2003.00503`.

[70] M. Cacciari and G. P. Salam, "Pileup subtraction using jet areas", *Phys. Lett. B* **659** (2008) 119, `doi:10.1016/j.physletb.2007.09.077.`, `arXiv:0707.1378`.

[71] CMS Collaboration, "Particle-flow reconstruction and global event description with the CMS detector", *JINST* **12** (2017) P10003, `doi:10.1088/1748-0221/12/10/p10003`, `arXiv:1706.04965`.

[72] CMS Collaboration, "Performance of electron reconstruction and selection with the CMS detector in proton-proton collisions at $\sqrt{s} = 8$ TeV", *JINST* **10** (2015) P06005, `doi:10.1088/1748-0221/10/06/P06005`, `arXiv:1502.02701`.

[73] CMS Collaboration, "Performance of the CMS muon detector and muon reconstruction with proton-proton collisions at $\sqrt{s} = 13$ TeV", *JINST* **13** (2018) P06015, `doi:10.1088/1748-0221/13/06/P06015`, `arXiv:1804.04528`.

[74] CMS Collaboration, "Description and performance of track and primary-vertex reconstruction with the CMS tracker", *JINST* **9** (2014) P10009, `doi:10.1088/1748-0221/9/10/p10009`, `arXiv:1405.6569`.

[75] CMS Collaboration, "Determination of jet energy calibration and transverse momentum resolution in CMS", *JINST* **6** (2011) P11002, `doi:10.1088/1748-0221/6/11/p11002`, `arXiv:1107.4277`.

[76] CMS Collaboration, "Jet energy scale and resolution in the CMS experiment in pp collisions at 8 TeV", *JINST* **12** (2017) P02014, `doi:10.1088/1748-0221/12/02/P02014`, `arXiv:1607.03663`.

[77] CMS Collaboration, "Performance of missing transverse momentum reconstruction in proton-proton collisions at $\sqrt{s} = 13$ TeV using the CMS detector", *JINST* **14** (2019) P07004, `doi:10.1088/1748-0221/14/07/P07004`, `arXiv:1903.06078`.

[78] CMS Collaboration, "Jet algorithms performance in 13 TeV data", CMS Physics Analysis Summary CMS-PAS-JME-16-003, 2017.

[79] A. Elagin, P. Murat, A. Pranko, and A. Safonov, "A new mass reconstruction technique for resonances decaying to $\tau\tau$", *Nucl. Instrum. Meth. A* **654** (2011) 481, `doi:10.1016/j.nima.2011.07.009`, `arXiv:1012.4686`.

[80] CMS Collaboration, "Search for new phenomena with multiple charged leptons in proton–proton collisions at $\sqrt{s} = 13$ TeV", *Eur. Phys. J. C* **77** (2017) 635, `doi:10.1140/epjc/s10052-017-5182-1`, `arXiv:1701.06940`.

[81] CMS Collaboration, "Measurement of the inelastic proton-proton cross section at $\sqrt{s} = 13\,\text{TeV}$", *JHEP* **07** (2018) `doi:10.1007/JHEP07(2018)161`, `arXiv:1802.02613`.

[82] CMS Collaboration, "CMS luminosity measurements for the 2016 data taking period", CMS Physics Analysis Summary CMS-PAS-LUM-17-001, 2017.

[83] CMS Collaboration, "CMS luminosity measurement for the 2017 data-taking period at $\sqrt{s} = 13\,\text{TeV}$", CMS Physics Analysis Summary CMS-PAS-LUM-17-004, 2018.

[84] CMS Collaboration, "CMS luminosity measurement for the 2018 data-taking period at $\sqrt{s} = 13\,\text{TeV}$", CMS Physics Analysis Summary CMS-PAS-LUM-18-002, 2019.

[85] T. Junk, "Confidence level computation for combining searches with small statistics", *Nucl. Instrum. Meth. A* **434** (1999) 435, `doi:10.1016/S0168-9002(99)00498-2`, `arXiv:hep-ex/9902006`.

[86] A. L. Read, "Presentation of search results: the CL_s technique", *J. Phys. G* **28** (2002) 2693, `doi:10.1088/0954-3899/28/10/313`.

[87] G. Cowan, K. Cranmer, E. Gross, and O. Vitells, "Asymptotic formulae for likelihood-based tests of new physics", *Eur. Phys. J. C* **71** (2011) 1554, `doi:10.1140/epjc/s10052-011-1554-0`, `arXiv:1007.1727`. [Erratum: `doi:10.1140/epjc/s10052-013-2501-z`].

[88] ATLAS and CMS Collaborations, LHC Higgs Combination Group, "Procedure for the LHC Higgs boson search combination in summer 2011", Technical Report ATL-PHYS-PUB/2011-11, CMS NOTE 2011/005, 2011.

A The CMS Collaboration

Yerevan Physics Institute, Yerevan, Armenia
A. Tumasyan

Institut für Hochenergiephysik, Vienna, Austria
W. Adam, J.W. Andrejkovic, T. Bergauer, S. Chatterjee, M. Dragicevic, A. Escalante Del Valle, R. Frühwirth[1], M. Jeitler[1], N. Krammer, L. Lechner, D. Liko, I. Mikulec, P. Paulitsch, F.M. Pitters, J. Schieck[1], R. Schöfbeck, M. Spanring, S. Templ, W. Waltenberger, C.-E. Wulz[1]

Institute for Nuclear Problems, Minsk, Belarus
V. Chekhovsky, A. Litomin, V. Makarenko

Universiteit Antwerpen, Antwerpen, Belgium
M.R. Darwish[2], E.A. De Wolf, T. Janssen, T. Kello[3], A. Lelek, H. Rejeb Sfar, P. Van Mechelen, S. Van Putte, N. Van Remortel

Vrije Universiteit Brussel, Brussel, Belgium
F. Blekman, E.S. Bols, J. D'Hondt, J. De Clercq, M. Delcourt, H. El Faham, S. Lowette, S. Moortgat, A. Morton, D. Müller, A.R. Sahasransu, S. Tavernier, W. Van Doninck, P. Van Mulders

Université Libre de Bruxelles, Bruxelles, Belgium
D. Beghin, B. Bilin, B. Clerbaux, G. De Lentdecker, L. Favart, A. Grebenyuk, A.K. Kalsi, K. Lee, M. Mahdavikhorrami, I. Makarenko, L. Moureaux, L. Pétré, A. Popov, N. Postiau, E. Starling, L. Thomas, M. Vanden Bemden, C. Vander Velde, P. Vanlaer, D. Vannerom, L. Wezenbeek

Ghent University, Ghent, Belgium
T. Cornelis, D. Dobur, J. Knolle, L. Lambrecht, G. Mestdach, M. Niedziela, C. Roskas, A. Samalan, K. Skovpen, M. Tytgat, W. Verbeke, B. Vermassen, M. Vit

Université Catholique de Louvain, Louvain-la-Neuve, Belgium
A. Bethani, G. Bruno, F. Bury, C. Caputo, P. David, C. Delaere, I.S. Donertas, A. Giammanco, K. Jaffel, Sa. Jain, V. Lemaitre, K. Mondal, J. Prisciandaro, A. Taliercio, M. Teklishyn, T.T. Tran, P. Vischia, S. Wertz

Centro Brasileiro de Pesquisas Fisicas, Rio de Janeiro, Brazil
G.A. Alves, C. Hensel, A. Moraes

Universidade do Estado do Rio de Janeiro, Rio de Janeiro, Brazil
W.L. Aldá Júnior, M. Alves Gallo Pereira, M. Barroso Ferreira Filho, H. BRANDAO MALBOUISSON, W. Carvalho, J. Chinellato[4], E.M. Da Costa, G.G. Da Silveira[5], D. De Jesus Damiao, S. Fonseca De Souza, D. Matos Figueiredo, C. Mora Herrera, K. Mota Amarilo, L. Mundim, H. Nogima, P. Rebello Teles, A. Santoro, S.M. Silva Do Amaral, A. Sznajder, M. Thiel, F. Torres Da Silva De Araujo, A. Vilela Pereira

Universidade Estadual Paulista (a), Universidade Federal do ABC (b), São Paulo, Brazil
C.A. Bernardes[5], L. Calligaris, T.R. Fernandez Perez Tomei, E.M. Gregores, D.S. Lemos, P.G. Mercadante, S.F. Novaes, Sandra S. Padula

Institute for Nuclear Research and Nuclear Energy, Bulgarian Academy of Sciences, Sofia, Bulgaria
A. Aleksandrov, G. Antchev, R. Hadjiiska, P. Iaydjiev, M. Misheva, M. Rodozov, M. Shopova,

G. Sultanov

University of Sofia, Sofia, Bulgaria
A. Dimitrov, T. Ivanov, L. Litov (iD), B. Pavlov, P. Petkov, A. Petrov

Beihang University, Beijing, China
T. Cheng (iD), Q. Guo, T. Javaid[6], M. Mittal, H. Wang, L. Yuan

Department of Physics, Tsinghua University, Beijing, China
M. Ahmad (iD), G. Bauer, C. Dozen[7] (iD), Z. Hu (iD), J. Martins[8] (iD), Y. Wang, K. Yi[9,10]

Institute of High Energy Physics, Beijing, China
E. Chapon (iD), G.M. Chen[6] (iD), H.S. Chen[6] (iD), M. Chen (iD), F. Iemmi, A. Kapoor (iD), D. Leggat, H. Liao, Z.-A. Liu[6] (iD), V. Milosevic (iD), F. Monti (iD), R. Sharma (iD), J. Tao (iD), J. Thomas-Wilsker, J. Wang (iD), H. Zhang (iD), S. Zhang[6], J. Zhao (iD)

State Key Laboratory of Nuclear Physics and Technology, Peking University, Beijing, China
A. Agapitos, Y. Ban, C. Chen, Q. Huang, A. Levin (iD), Q. Li (iD), X. Lyu, Y. Mao, S.J. Qian, D. Wang (iD), Q. Wang (iD), J. Xiao

Sun Yat-Sen University, Guangzhou, China
M. Lu, Z. You (iD)

Institute of Modern Physics and Key Laboratory of Nuclear Physics and Ion-beam Application (MOE) - Fudan University, Shanghai, China
X. Gao[3], H. Okawa (iD)

Zhejiang University, Hangzhou, China, Zhejiang, China
Z. Lin (iD), M. Xiao (iD)

Universidad de Los Andes, Bogota, Colombia
C. Avila (iD), A. Cabrera (iD), C. Florez (iD), J. Fraga, A. Sarkar (iD), M.A. Segura Delgado

Universidad de Antioquia, Medellin, Colombia
J. Mejia Guisao, F. Ramirez, J.D. Ruiz Alvarez (iD), C.A. Salazar González (iD)

University of Split, Faculty of Electrical Engineering, Mechanical Engineering and Naval Architecture, Split, Croatia
D. Giljanovic, N. Godinovic (iD), D. Lelas (iD), I. Puljak (iD)

University of Split, Faculty of Science, Split, Croatia
Z. Antunovic, M. Kovac, T. Sculac (iD)

Institute Rudjer Boskovic, Zagreb, Croatia
V. Brigljevic (iD), D. Ferencek (iD), D. Majumder (iD), M. Roguljic, A. Starodumov[11] (iD), T. Susa (iD)

University of Cyprus, Nicosia, Cyprus
A. Attikis (iD), K. Christoforou, E. Erodotou, A. Ioannou, G. Kole (iD), M. Kolosova, S. Konstantinou, J. Mousa (iD), C. Nicolaou, F. Ptochos (iD), P.A. Razis, H. Rykaczewski, H. Saka (iD)

Charles University, Prague, Czech Republic
M. Finger[12], M. Finger Jr.[12] (iD), A. Kveton

Escuela Politecnica Nacional, Quito, Ecuador
E. Ayala

Universidad San Francisco de Quito, Quito, Ecuador
E. Carrera Jarrin (iD)

Academy of Scientific Research and Technology of the Arab Republic of Egypt, Egyptian Network of High Energy Physics, Cairo, Egypt
H. Abdalla[13] ⓘD, S. Khalil[14] ⓘD

Center for High Energy Physics (CHEP-FU), Fayoum University, El-Fayoum, Egypt
A. Lotfy ⓘD, M.A. Mahmoud ⓘD

National Institute of Chemical Physics and Biophysics, Tallinn, Estonia
S. Bhowmik ⓘD, R.K. Dewanjee ⓘD, K. Ehataht, M. Kadastik, S. Nandan, C. Nielsen, J. Pata, M. Raidal ⓘD, L. Tani, C. Veelken

Department of Physics, University of Helsinki, Helsinki, Finland
P. Eerola ⓘD, L. Forthomme ⓘD, H. Kirschenmann ⓘD, K. Osterberg ⓘD, M. Voutilainen ⓘD

Helsinki Institute of Physics, Helsinki, Finland
S. Bharthuar, E. Brücken ⓘD, F. Garcia ⓘD, J. Havukainen ⓘD, M.S. Kim ⓘD, R. Kinnunen, T. Lampén, K. Lassila-Perini ⓘD, S. Lehti ⓘD, T. Lindén, M. Lotti, L. Martikainen, M. Myllymäki, J. Ott ⓘD, H. Siikonen, E. Tuominen ⓘD, J. Tuominiemi

Lappeenranta University of Technology, Lappeenranta, Finland
P. Luukka ⓘD, H. Petrow, T. Tuuva

IRFU, CEA, Université Paris-Saclay, Gif-sur-Yvette, France
C. Amendola ⓘD, M. Besancon, F. Couderc ⓘD, M. Dejardin, D. Denegri, J.L. Faure, F. Ferri ⓘD, S. Ganjour, A. Givernaud, P. Gras, G. Hamel de Monchenault ⓘD, P. Jarry, B. Lenzi ⓘD, E. Locci, J. Malcles, J. Rander, A. Rosowsky ⓘD, M.Ö. Sahin ⓘD, A. Savoy-Navarro[15], M. Titov ⓘD, G.B. Yu ⓘD

Laboratoire Leprince-Ringuet, CNRS/IN2P3, Ecole Polytechnique, Institut Polytechnique de Paris, Palaiseau, France
S. Ahuja ⓘD, F. Beaudette ⓘD, M. Bonanomi ⓘD, A. Buchot Perraguin, P. Busson, A. Cappati, C. Charlot, O. Davignon, B. Diab, G. Falmagne ⓘD, S. Ghosh, R. Granier de Cassagnac ⓘD, A. Hakimi, I. Kucher ⓘD, M. Nguyen ⓘD, C. Ochando ⓘD, P. Paganini ⓘD, J. Rembser, R. Salerno ⓘD, J.B. Sauvan ⓘD, Y. Sirois ⓘD, A. Zabi, A. Zghiche ⓘD

Université de Strasbourg, CNRS, IPHC UMR 7178, Strasbourg, France
J.-L. Agram[16] ⓘD, J. Andrea, D. Apparu, D. Bloch ⓘD, G. Bourgatte, J.-M. Brom, E.C. Chabert, C. Collard ⓘD, D. Darej, J.-C. Fontaine[16], U. Goerlach, C. Grimault, A.-C. Le Bihan, E. Nibigira ⓘD, P. Van Hove ⓘD

Institut de Physique des 2 Infinis de Lyon (IP2I), Villeurbanne, France
E. Asilar ⓘD, S. Beauceron ⓘD, C. Bernet ⓘD, G. Boudoul, C. Camen, A. Carle, N. Chanon ⓘD, D. Contardo, P. Depasse ⓘD, H. El Mamouni, J. Fay, S. Gascon ⓘD, M. Gouzevitch ⓘD, B. Ille, I.B. Laktineh, H. Lattaud ⓘD, A. Lesauvage ⓘD, M. Lethuillier ⓘD, L. Mirabito, S. Perries, K. Shchablo, V. Sordini ⓘD, L. Torterotot ⓘD, G. Touquet, M. Vander Donckt, S. Viret

Georgian Technical University, Tbilisi, Georgia
A. Khvedelidze[12] ⓘD, I. Lomidze, Z. Tsamalaidze[12]

RWTH Aachen University, I. Physikalisches Institut, Aachen, Germany
L. Feld ⓘD, K. Klein, M. Lipinski, D. Meuser, A. Pauls, M.P. Rauch, N. Röwert, J. Schulz, M. Teroerde ⓘD

RWTH Aachen University, III. Physikalisches Institut A, Aachen, Germany
A. Dodonova, D. Eliseev, M. Erdmann ⓘD, P. Fackeldey ⓘD, B. Fischer, S. Ghosh ⓘD, T. Hebbeker ⓘD, K. Hoepfner, F. Ivone, H. Keller, L. Mastrolorenzo, M. Merschmeyer ⓘD,

A. Meyer ⓘ, G. Mocellin, S. Mondal, S. Mukherjee ⓘ, D. Noll ⓘ, A. Novak, T. Pook ⓘ, A. Pozdnyakov ⓘ, Y. Rath, H. Reithler, J. Roemer, A. Schmidt ⓘ, S.C. Schuler, A. Sharma ⓘ, L. Vigilante, S. Wiedenbeck, S. Zaleski

RWTH Aachen University, III. Physikalisches Institut B, Aachen, Germany
C. Dziwok, G. Flügge, W. Haj Ahmad[17] ⓘ, O. Hlushchenko, T. Kress, A. Nowack ⓘ, C. Pistone, O. Pooth, D. Roy ⓘ, H. Sert ⓘ, A. Stahl[18] ⓘ, T. Ziemons ⓘ

Deutsches Elektronen-Synchrotron, Hamburg, Germany
H. Aarup Petersen, M. Aldaya Martin, P. Asmuss, I. Babounikau ⓘ, S. Baxter, O. Behnke, A. Bermúdez Martínez, S. Bhattacharya, A.A. Bin Anuar ⓘ, K. Borras[19], V. Botta, D. Brunner, A. Campbell ⓘ, A. Cardini ⓘ, C. Cheng, F. Colombina, S. Consuegra Rodríguez ⓘ, G. Correia Silva, V. Danilov, L. Didukh, G. Eckerlin, D. Eckstein, L.I. Estevez Banos ⓘ, O. Filatov ⓘ, E. Gallo[20], A. Geiser, A. Giraldi, A. Grohsjean ⓘ, M. Guthoff, A. Jafari[21] ⓘ, N.Z. Jomhari ⓘ, H. Jung ⓘ, A. Kasem[19] ⓘ, M. Kasemann ⓘ, H. Kaveh ⓘ, C. Kleinwort ⓘ, D. Krücker ⓘ, W. Lange, J. Lidrych ⓘ, K. Lipka, W. Lohmann[22], R. Mankel, I.-A. Melzer-Pellmann ⓘ, J. Metwally, A.B. Meyer ⓘ, M. Meyer ⓘ, J. Mnich ⓘ, A. Mussgiller, Y. Otarid, D. Pérez Adán ⓘ, D. Pitzl, A. Raspereza, B. Ribeiro Lopes, J. Rübenach, A. Saggio ⓘ, A. Saibel ⓘ, M. Savitskyi ⓘ, M. Scham, V. Scheurer, C. Schwanenberger[20] ⓘ, A. Singh, R.E. Sosa Ricardo ⓘ, D. Stafford, N. Tonon ⓘ, O. Turkot ⓘ, M. Van De Klundert ⓘ, R. Walsh ⓘ, D. Walter, Y. Wen ⓘ, K. Wichmann, L. Wiens, C. Wissing, S. Wuchterl ⓘ

University of Hamburg, Hamburg, Germany
R. Aggleton, S. Albrecht ⓘ, S. Bein ⓘ, L. Benato ⓘ, A. Benecke, P. Connor ⓘ, K. De Leo ⓘ, M. Eich, F. Feindt, A. Fröhlich, C. Garbers ⓘ, E. Garutti ⓘ, P. Gunnellini, J. Haller ⓘ, A. Hinzmann ⓘ, G. Kasieczka, R. Klanner ⓘ, R. Kogler ⓘ, T. Kramer, V. Kutzner, J. Lange ⓘ, T. Lange ⓘ, A. Lobanov ⓘ, A. Malara ⓘ, A. Nigamova, K.J. Pena Rodriguez, O. Rieger, P. Schleper, M. Schröder ⓘ, J. Schwandt ⓘ, D. Schwarz, J. Sonneveld ⓘ, H. Stadie, G. Steinbrück, A. Tews, B. Vormwald ⓘ, I. Zoi ⓘ

Karlsruher Institut fuer Technologie, Karlsruhe, Germany
J. Bechtel ⓘ, T. Berger, E. Butz ⓘ, R. Caspart ⓘ, T. Chwalek, W. De Boer[†], A. Dierlamm, A. Droll, K. El Morabit, N. Faltermann ⓘ, M. Giffels, J.o. Gosewisch, A. Gottmann, F. Hartmann[18] ⓘ, C. Heidecker, U. Husemann ⓘ, I. Katkov[23], P. Keicher, R. Koppenhöfer, S. Maier, M. Metzler, S. Mitra ⓘ, Th. Müller, M. Neukum, A. Nürnberg, G. Quast ⓘ, K. Rabbertz ⓘ, J. Rauser, D. Savoiu ⓘ, M. Schnepf, D. Seith, I. Shvetsov, H.J. Simonis, R. Ulrich ⓘ, J. Van Der Linden, R.F. Von Cube, M. Wassmer, M. Weber ⓘ, S. Wieland, R. Wolf ⓘ, S. Wozniewski, S. Wunsch

Institute of Nuclear and Particle Physics (INPP), NCSR Demokritos, Aghia Paraskevi, Greece
G. Anagnostou, G. Daskalakis, T. Geralis ⓘ, A. Kyriakis, D. Loukas, A. Stakia ⓘ

National and Kapodistrian University of Athens, Athens, Greece
M. Diamantopoulou, D. Karasavvas, G. Karathanasis, P. Kontaxakis ⓘ, C.K. Koraka, A. Manousakis-Katsikakis, A. Panagiotou, I. Papavergou, N. Saoulidou ⓘ, K. Theofilatos ⓘ, E. Tziaferi ⓘ, K. Vellidis, E. Vourliotis

National Technical University of Athens, Athens, Greece
G. Bakas, K. Kousouris ⓘ, I. Papakrivopoulos, G. Tsipolitis, A. Zacharopoulou

University of Ioánnina, Ioánnina, Greece
I. Evangelou ⓘ, C. Foudas, P. Gianneios, P. Katsoulis, P. Kokkas, N. Manthos, I. Papadopoulos ⓘ, J. Strologas ⓘ

MTA-ELTE Lendület CMS Particle and Nuclear Physics Group, Eötvös Loránd University, Budapest, Hungary

M. Csanad [iD], K. Farkas, M.M.A. Gadallah[24] [iD], S. Lökös[25] [iD], P. Major, K. Mandal [iD], A. Mehta [iD], G. Pasztor [iD], A.J. Rádl, O. Surányi, G.I. Veres [iD]

Wigner Research Centre for Physics, Budapest, Hungary

M. Bartók[26] [iD], G. Bencze, C. Hajdu [iD], D. Horvath[27] [iD], F. Sikler [iD], V. Veszpremi [iD], G. Vesztergombi[†]

Institute of Nuclear Research ATOMKI, Debrecen, Hungary

S. Czellar, J. Karancsi[26] [iD], J. Molnar, Z. Szillasi, D. Teyssier

Institute of Physics, University of Debrecen, Debrecen, Hungary

P. Raics, Z.L. Trocsanyi[28] [iD], B. Ujvari

Karoly Robert Campus, MATE Institute of Technology, Gyongyos, Hungary

T. Csorgo[29] [iD], F. Nemes[29], T. Novak

Indian Institute of Science (IISc), Bangalore, India

J.R. Komaragiri [iD], D. Kumar, L. Panwar [iD], P.C. Tiwari [iD]

National Institute of Science Education and Research, HBNI, Bhubaneswar, India

S. Bahinipati[30] [iD], C. Kar [iD], P. Mal, T. Mishra [iD], V.K. Muraleedharan Nair Bindhu[31], A. Nayak[31] [iD], P. Saha, N. Sur [iD], S.K. Swain, D. Vats[31]

Panjab University, Chandigarh, India

S. Bansal [iD], S.B. Beri, V. Bhatnagar [iD], G. Chaudhary [iD], S. Chauhan [iD], N. Dhingra[32] [iD], R. Gupta, A. Kaur, M. Kaur [iD], S. Kaur, P. Kumari [iD], M. Meena, K. Sandeep [iD], J.B. Singh [iD], A.K. Virdi [iD]

University of Delhi, Delhi, India

A. Ahmed, A. Bhardwaj [iD], B.C. Choudhary [iD], M. Gola, S. Keshri [iD], A. Kumar [iD], M. Naimuddin [iD], P. Priyanka [iD], K. Ranjan, A. Shah [iD]

Saha Institute of Nuclear Physics, HBNI, Kolkata, India

M. Bharti[33], R. Bhattacharya, S. Bhattacharya [iD], D. Bhowmik, S. Dutta, S. Dutta, B. Gomber[34] [iD], M. Maity[35], P. Palit [iD], P.K. Rout [iD], G. Saha, B. Sahu [iD], S. Sarkar, M. Sharan, B. Singh[33], S. Thakur[33]

Indian Institute of Technology Madras, Madras, India

P.K. Behera [iD], S.C. Behera, P. Kalbhor [iD], A. Muhammad, R. Pradhan, P.R. Pujahari, A. Sharma [iD], A.K. Sikdar

Bhabha Atomic Research Centre, Mumbai, India

D. Dutta [iD], V. Jha, V. Kumar [iD], D.K. Mishra, K. Naskar[36], P.K. Netrakanti, L.M. Pant, P. Shukla [iD]

Tata Institute of Fundamental Research-A, Mumbai, India

T. Aziz, S. Dugad, M. Kumar, U. Sarkar [iD]

Tata Institute of Fundamental Research-B, Mumbai, India

S. Banerjee [iD], R. Chudasama, M. Guchait, S. Karmakar, S. Kumar, G. Majumder, K. Mazumdar, S. Mukherjee [iD]

Indian Institute of Science Education and Research (IISER), Pune, India

K. Alpana, S. Dube [iD], B. Kansal, A. Laha, S. Pandey [iD], A. Rane [iD], A. Rastogi [iD], S. Sharma [iD]

Isfahan University of Technology, Isfahan, Iran
H. Bakhshiansohi[37] (iD), M. Zeinali[38]

Institute for Research in Fundamental Sciences (IPM), Tehran, Iran
S. Chenarani[39], S.M. Etesami (iD), M. Khakzad (iD), M. Mohammadi Najafabadi (iD)

University College Dublin, Dublin, Ireland
M. Grunewald (iD)

INFN Sezione di Bari [a], Bari, Italy, Università di Bari [b], Bari, Italy, Politecnico di Bari [c], Bari, Italy
M. Abbrescia[a,b] (iD), R. Aly[a,b,40] (iD), C. Aruta[a,b], A. Colaleo[a] (iD), D. Creanza[a,c] (iD), N. De Filippis[a,c] (iD), M. De Palma[a,b] (iD), A. Di Florio[a,b], A. Di Pilato[a,b] (iD), W. Elmetenawee[a,b] (iD), L. Fiore[a] (iD), A. Gelmi[a,b] (iD), M. Gul[a] (iD), G. Iaselli[a,c] (iD), M. Ince[a,b] (iD), S. Lezki[a,b] (iD), G. Maggi[a,c] (iD), M. Maggi[a] (iD), I. Margjeka[a,b], V. Mastrapasqua[a,b] (iD), J.A. Merlin[a], S. My[a,b] (iD), S. Nuzzo[a,b] (iD), A. Pellecchia[a,b], A. Pompili[a,b] (iD), G. Pugliese[a,c] (iD), A. Ranieri[a] (iD), G. Selvaggi[a,b] (iD), L. Silvestris[a] (iD), F.M. Simone[a,b] (iD), R. Venditti[a] (iD), P. Verwilligen[a] (iD)

INFN Sezione di Bologna [a], Bologna, Italy, Università di Bologna [b], Bologna, Italy
G. Abbiendi[a] (iD), C. Battilana[a,b] (iD), D. Bonacorsi[a,b] (iD), L. Borgonovi[a], L. Brigliadori[a], R. Campanini[a,b] (iD), P. Capiluppi[a,b] (iD), A. Castro[a,b] (iD), F.R. Cavallo[a] (iD), M. Cuffiani[a,b] (iD), G.M. Dallavalle[a] (iD), T. Diotalevi[a,b] (iD), F. Fabbri[a] (iD), A. Fanfani[a,b] (iD), P. Giacomelli[a] (iD), L. Giommi[a,b] (iD), C. Grandi[a] (iD), L. Guiducci[a,b], S. Lo Meo[a,41], L. Lunerti[a,b], S. Marcellini[a] (iD), G. Masetti[a] (iD), F.L. Navarria[a,b] (iD), A. Perrotta[a] (iD), F. Primavera[a,b] (iD), A.M. Rossi[a,b] (iD), T. Rovelli[a,b] (iD), G.P. Siroli[a,b] (iD)

INFN Sezione di Catania [a], Catania, Italy, Università di Catania [b], Catania, Italy
S. Albergo[a,b,42] (iD), S. Costa[a,b,42] (iD), A. Di Mattia[a] (iD), R. Potenza[a,b], A. Tricomi[a,b,42] (iD), C. Tuve[a,b] (iD)

INFN Sezione di Firenze [a], Firenze, Italy, Università di Firenze [b], Firenze, Italy
G. Barbagli[a] (iD), A. Cassese[a] (iD), R. Ceccarelli[a,b], V. Ciulli[a,b] (iD), C. Civinini[a] (iD), R. D'Alessandro[a,b] (iD), E. Focardi[a,b] (iD), G. Latino[a,b] (iD), P. Lenzi[a,b] (iD), M. Lizzo[a,b], M. Meschini[a] (iD), S. Paoletti[a] (iD), R. Seidita[a,b], G. Sguazzoni[a] (iD), L. Viliani[a] (iD)

INFN Laboratori Nazionali di Frascati, Frascati, Italy
L. Benussi (iD), S. Bianco (iD), D. Piccolo (iD)

INFN Sezione di Genova [a], Genova, Italy, Università di Genova [b], Genova, Italy
M. Bozzo[a,b] (iD), F. Ferro[a] (iD), R. Mulargia[a,b], E. Robutti[a] (iD), S. Tosi[a,b] (iD)

INFN Sezione di Milano-Bicocca [a], Milano, Italy, Università di Milano-Bicocca [b], Milano, Italy
A. Benaglia[a] (iD), F. Brivio[a,b], F. Cetorelli[a,b], V. Ciriolo[a,b,18], F. De Guio[a,b] (iD), M.E. Dinardo[a,b] (iD), P. Dini[a] (iD), S. Gennai[a] (iD), A. Ghezzi[a,b] (iD), P. Govoni[a,b] (iD), L. Guzzi[a,b] (iD), M. Malberti[a], S. Malvezzi[a] (iD), A. Massironi[a] (iD), D. Menasce[a] (iD), L. Moroni[a] (iD), M. Paganoni[a,b] (iD), D. Pedrini[a] (iD), S. Ragazzi[a,b] (iD), N. Redaelli[a] (iD), T. Tabarelli de Fatis[a,b] (iD), D. Valsecchi[a,b,18], D. Zuolo[a,b] (iD)

INFN Sezione di Napoli [a], Napoli, Italy, Università di Napoli 'Federico II' [b], Napoli, Italy, Università della Basilicata [c], Potenza, Italy, Università G. Marconi [d], Roma, Italy
S. Buontempo[a] (iD), F. Carnevali[a,b], N. Cavallo[a,c] (iD), A. De Iorio[a,b] (iD), F. Fabozzi[a,c] (iD), A.O.M. Iorio[a,b] (iD), L. Lista[a,b] (iD), S. Meola[a,d,18] (iD), P. Paolucci[a,18] (iD), B. Rossi[a] (iD), C. Sciacca[a,b] (iD)

INFN Sezione di Padova [a], Padova, Italy, Università di Padova [b], Padova, Italy, Università

di Trento [c], Trento, Italy

P. Azzi[a] (iD), N. Bacchetta[a] (iD), D. Bisello[a,b] (iD), P. Bortignon[a] (iD), A. Bragagnolo[a,b] (iD), R. Carlin[a,b] (iD), P. Checchia[a] (iD), T. Dorigo[a] (iD), U. Dosselli[a] (iD), F. Gasparini[a,b] (iD), U. Gasparini[a,b] (iD), S.Y. Hoh[a,b] (iD), L. Layer[a,43], M. Margoni[a,b] (iD), A.T. Meneguzzo[a,b] (iD), J. Pazzini[a,b] (iD), M. Presilla[a,b] (iD), P. Ronchese[a,b] (iD), R. Rossin[a,b], F. Simonetto[a,b] (iD), G. Strong[a] (iD), M. Tosi[a,b] (iD), H. YARAR[a,b], M. Zanetti[a,b] (iD), P. Zotto[a,b] (iD), A. Zucchetta[a,b] (iD), G. Zumerle[a,b] (iD)

INFN Sezione di Pavia [a], Pavia, Italy, Università di Pavia [b], Pavia, Italy

C. Aime'[a,b], A. Braghieri[a] (iD), S. Calzaferri[a,b], D. Fiorina[a,b] (iD), P. Montagna[a,b], S.P. Ratti[a,b], V. Re[a] (iD), C. Riccardi[a,b] (iD), P. Salvini[a] (iD), I. Vai[a] (iD), P. Vitulo[a,b] (iD)

INFN Sezione di Perugia [a], Perugia, Italy, Università di Perugia [b], Perugia, Italy

P. Asenov[a,44] (iD), G.M. Bilei[a] (iD), D. Ciangottini[a,b] (iD), L. Fanò[a,b] (iD), P. Lariccia[a,b], M. Magherini[b], G. Mantovani[a,b], V. Mariani[a,b], M. Menichelli[a] (iD), F. Moscatelli[a,44] (iD), A. Piccinelli[a,b] (iD), A. Rossi[a,b] (iD), A. Santocchia[a,b] (iD), D. Spiga[a] (iD), T. Tedeschi[a,b] (iD)

INFN Sezione di Pisa [a], Pisa, Italy, Università di Pisa [b], Pisa, Italy, Scuola Normale Superiore di Pisa [c], Pisa, Italy, Università di Siena [d], Siena, Italy

P. Azzurri[a] (iD), G. Bagliesi[a] (iD), V. Bertacchi[a,c] (iD), L. Bianchini[a] (iD), T. Boccali[a] (iD), E. Bossini[a,b] (iD), R. Castaldi[a] (iD), M.A. Ciocci[a,b] (iD), V. D'Amante[a,d] (iD), R. Dell'Orso[a] (iD), M.R. Di Domenico[a,d] (iD), S. Donato[a] (iD), A. Giassi[a] (iD), F. Ligabue[a,c] (iD), E. Manca[a,c] (iD), G. Mandorli[a,c] (iD), A. Messineo[a,b] (iD), F. Palla[a] (iD), S. Parolia[a,b], G. Ramirez-Sanchez[a,c], A. Rizzi[a,b] (iD), G. Rolandi[a,c] (iD), S. Roy Chowdhury[a,c], A. Scribano[a], N. Shafiei[a,b] (iD), P. Spagnolo[a] (iD), R. Tenchini[a] (iD), G. Tonelli[a,b] (iD), N. Turini[a,d] (iD), A. Venturi[a] (iD), P.G. Verdini[a] (iD)

INFN Sezione di Roma [a], Rome, Italy, Sapienza Università di Roma [b], Rome, Italy

M. Campana[a,b], F. Cavallari[a] (iD), D. Del Re[a,b] (iD), E. Di Marco[a] (iD), M. Diemoz[a] (iD), E. Longo[a,b] (iD), P. Meridiani[a] (iD), G. Organtini[a,b] (iD), F. Pandolfi[a], R. Paramatti[a,b] (iD), C. Quaranta[a,b], S. Rahatlou[a,b] (iD), C. Rovelli[a] (iD), F. Santanastasio[a,b] (iD), L. Soffi[a] (iD), R. Tramontano[a,b]

INFN Sezione di Torino [a], Torino, Italy, Università di Torino [b], Torino, Italy, Università del Piemonte Orientale [c], Novara, Italy

N. Amapane[a,b] (iD), R. Arcidiacono[a,c] (iD), S. Argiro[a,b] (iD), M. Arneodo[a,c] (iD), N. Bartosik[a] (iD), R. Bellan[a,b] (iD), A. Bellora[a,b] (iD), J. Berenguer Antequera[a,b] (iD), C. Biino[a] (iD), N. Cartiglia[a] (iD), S. Cometti[a] (iD), M. Costa[a,b] (iD), R. Covarelli[a,b] (iD), N. Demaria[a] (iD), B. Kiani[a,b] (iD), F. Legger[a] (iD), C. Mariotti[a] (iD), S. Maselli[a] (iD), E. Migliore[a,b] (iD), E. Monteil[a,b] (iD), M. Monteno[a] (iD), M.M. Obertino[a,b] (iD), G. Ortona[a] (iD), L. Pacher[a,b] (iD), N. Pastrone[a] (iD), M. Pelliccioni[a] (iD), G.L. Pinna Angioni[a,b], M. Ruspa[a,c] (iD), K. Shchelina[a,b] (iD), F. Siviero[a,b] (iD), V. Sola[a] (iD), A. Solano[a,b] (iD), D. Soldi[a,b] (iD), A. Staiano[a] (iD), M. Tornago[a,b], D. Trocino[a,b] (iD), A. Vagnerini

INFN Sezione di Trieste [a], Trieste, Italy, Università di Trieste [b], Trieste, Italy

S. Belforte[a] (iD), V. Candelise[a,b] (iD), M. Casarsa[a] (iD), F. Cossutti[a] (iD), A. Da Rold[a,b] (iD), G. Della Ricca[a,b] (iD), G. Sorrentino[a,b], F. Vazzoler[a,b] (iD)

Kyungpook National University, Daegu, Korea

S. Dogra (iD), C. Huh (iD), B. Kim, D.H. Kim (iD), G.N. Kim (iD), J. Kim, J. Lee, S.W. Lee (iD), C.S. Moon (iD), Y.D. Oh (iD), S.I. Pak, B.C. Radburn-Smith, S. Sekmen (iD), Y.C. Yang

Chonnam National University, Institute for Universe and Elementary Particles, Kwangju, Korea

H. Kim (iD), D.H. Moon (iD)

Hanyang University, Seoul, Korea

B. Francois [ID], T.J. Kim [ID], J. Park [ID]

Korea University, Seoul, Korea
S. Cho, S. Choi [ID], Y. Go, B. Hong [ID], K. Lee, K.S. Lee [ID], J. Lim, J. Park, S.K. Park, J. Yoo

Kyung Hee University, Department of Physics, Seoul, Republic of Korea, Seoul, Korea
J. Goh [ID], A. Gurtu

Sejong University, Seoul, Korea
H.S. Kim [ID], Y. Kim

Seoul National University, Seoul, Korea
J. Almond, J.H. Bhyun, J. Choi, S. Jeon, J. Kim, J.S. Kim, S. Ko, H. Kwon, H. Lee [ID], S. Lee, B.H. Oh, M. Oh [ID], S.B. Oh, H. Seo [ID], U.K. Yang, I. Yoon [ID]

University of Seoul, Seoul, Korea
W. Jang, D. Jeon, D.Y. Kang, Y. Kang, J.H. Kim, S. Kim, B. Ko, J.S.H. Lee [ID], Y. Lee, I.C. Park, Y. Roh, M.S. Ryu, D. Song, I.J. Watson [ID], S. Yang

Yonsei University, Department of Physics, Seoul, Korea
S. Ha, H.D. Yoo

Sungkyunkwan University, Suwon, Korea
M. Choi, Y. Jeong, H. Lee, Y. Lee, I. Yu [ID]

College of Engineering and Technology, American University of the Middle East (AUM), Egaila, Kuwait, Dasman, Kuwait
T. Beyrouthy, Y. Maghrbi

Riga Technical University, Riga, Latvia
T. Torims, V. Veckalns[45] [ID]

Vilnius University, Vilnius, Lithuania
M. Ambrozas, A. Carvalho Antunes De Oliveira [ID], A. Juodagalvis [ID], A. Rinkevicius [ID], G. Tamulaitis [ID]

National Centre for Particle Physics, Universiti Malaya, Kuala Lumpur, Malaysia
N. Bin Norjoharuddeen [ID], W.A.T. Wan Abdullah, M.N. Yusli, Z. Zolkapli

Universidad de Sonora (UNISON), Hermosillo, Mexico
J.F. Benitez [ID], A. Castaneda Hernandez [ID], M. León Coello, J.A. Murillo Quijada [ID], A. Sehrawat, L. Valencia Palomo [ID]

Centro de Investigacion y de Estudios Avanzados del IPN, Mexico City, Mexico
G. Ayala, H. Castilla-Valdez, E. De La Cruz-Burelo [ID], I. Heredia-De La Cruz[46] [ID], R. Lopez-Fernandez, C.A. Mondragon Herrera, D.A. Perez Navarro, A. Sánchez Hernández [ID]

Universidad Iberoamericana, Mexico City, Mexico
S. Carrillo Moreno, C. Oropeza Barrera [ID], M. Ramírez García [ID], F. Vazquez Valencia

Benemerita Universidad Autonoma de Puebla, Puebla, Mexico
I. Pedraza, H.A. Salazar Ibarguen, C. Uribe Estrada

University of Montenegro, Podgorica, Montenegro
J. Mijuskovic[47], N. Raicevic

University of Auckland, Auckland, New Zealand
D. Krofcheck [ID]

University of Canterbury, Christchurch, New Zealand
S. Bheesette, P.H. Butler

National Centre for Physics, Quaid-I-Azam University, Islamabad, Pakistan
A. Ahmad, M.I. Asghar, A. Awais, M.I.M. Awan, H.R. Hoorani, W.A. Khan, M.A. Shah, M. Shoaib , M. Waqas

AGH University of Science and Technology Faculty of Computer Science, Electronics and Telecommunications, Krakow, Poland
V. Avati, L. Grzanka, M. Malawski

National Centre for Nuclear Research, Swierk, Poland
H. Bialkowska, M. Bluj , B. Boimska , M. Górski, M. Kazana, M. Szleper , P. Zalewski

Institute of Experimental Physics, Faculty of Physics, University of Warsaw, Warsaw, Poland
K. Bunkowski, K. Doroba, A. Kalinowski , M. Konecki , J. Krolikowski , M. Walczak

Laboratório de Instrumentação e Física Experimental de Partículas, Lisboa, Portugal
M. Araujo, P. Bargassa , D. Bastos, A. Boletti , P. Faccioli , M. Gallinaro , J. Hollar , N. Leonardo , T. Niknejad, M. Pisano, J. Seixas , O. Toldaiev , J. Varela

Joint Institute for Nuclear Research, Dubna, Russia
S. Afanasiev, D. Budkouski, I. Golutvin, I. Gorbunov , V. Karjavine, V. Korenkov , A. Lanev, A. Malakhov, V. Matveev[48,49], V. Palichik, V. Perelygin, M. Savina, D. Seitova, V. Shalaev, S. Shmatov, S. Shulha, V. Smirnov, O. Teryaev, N. Voytishin, B.S. Yuldashev[50], A. Zarubin, I. Zhizhin

Petersburg Nuclear Physics Institute, Gatchina (St. Petersburg), Russia
G. Gavrilov , V. Golovtcov, Y. Ivanov, V. Kim[51] , E. Kuznetsova[52], V. Murzin, V. Oreshkin, I. Smirnov, D. Sosnov , V. Sulimov, L. Uvarov, S. Volkov, A. Vorobyev

Institute for Nuclear Research, Moscow, Russia
Yu. Andreev , A. Dermenev, S. Gninenko , N. Golubev, A. Karneyeu , D. Kirpichnikov , M. Kirsanov, N. Krasnikov, A. Pashenkov, G. Pivovarov , D. Tlisov[†], A. Toropin

Institute for Theoretical and Experimental Physics named by A.I. Alikhanov of NRC 'Kurchatov Institute', Moscow, Russia
V. Epshteyn, V. Gavrilov, N. Lychkovskaya, A. Nikitenko[53], V. Popov, A. Spiridonov, A. Stepennov, M. Toms, E. Vlasov , A. Zhokin

Moscow Institute of Physics and Technology, Moscow, Russia
T. Aushev

National Research Nuclear University 'Moscow Engineering Physics Institute' (MEPhI), Moscow, Russia
R. Chistov[54] , M. Danilov[55] , A. Oskin, P. Parygin, S. Polikarpov[55]

P.N. Lebedev Physical Institute, Moscow, Russia
V. Andreev, M. Azarkin, I. Dremin , M. Kirakosyan, A. Terkulov

Skobeltsyn Institute of Nuclear Physics, Lomonosov Moscow State University, Moscow, Russia
A. Belyaev, E. Boos , V. Bunichev, M. Dubinin[56] , L. Dudko , A. Ershov, A. Gribushin, V. Klyukhin , O. Kodolova , I. Lokhtin , S. Obraztsov, M. Perfilov, V. Savrin

Novosibirsk State University (NSU), Novosibirsk, Russia

V. Blinov[57], T. Dimova[57], L. Kardapoltsev[57], A. Kozyrev[57], I. Ovtin[57], Y. Skovpen[57] (iD)

Institute for High Energy Physics of National Research Centre 'Kurchatov Institute', Protvino, Russia
I. Azhgirey (iD), I. Bayshev, D. Elumakhov, V. Kachanov, D. Konstantinov (iD), P. Mandrik (iD), V. Petrov, R. Ryutin, S. Slabospitskii (iD), A. Sobol, S. Troshin (iD), N. Tyurin, A. Uzunian, A. Volkov

National Research Tomsk Polytechnic University, Tomsk, Russia
A. Babaev, V. Okhotnikov

Tomsk State University, Tomsk, Russia
V. Borshch, V. Ivanchenko (iD), E. Tcherniaev (iD)

University of Belgrade: Faculty of Physics and VINCA Institute of Nuclear Sciences, Belgrade, Serbia
P. Adzic[58] (iD), M. Dordevic (iD), P. Milenovic (iD), J. Milosevic (iD)

Centro de Investigaciones Energéticas Medioambientales y Tecnológicas (CIEMAT), Madrid, Spain
M. Aguilar-Benitez, J. Alcaraz Maestre (iD), A. Álvarez Fernández, I. Bachiller, M. Barrio Luna, Cristina F. Bedoya (iD), C.A. Carrillo Montoya (iD), M. Cepeda (iD), M. Cerrada, N. Colino (iD), B. De La Cruz, A. Delgado Peris (iD), J.P. Fernández Ramos (iD), J. Flix (iD), M.C. Fouz (iD), O. Gonzalez Lopez (iD), S. Goy Lopez (iD), J.M. Hernandez (iD), M.I. Josa (iD), J. León Holgado (iD), D. Moran, Á. Navarro Tobar (iD), A. Pérez-Calero Yzquierdo (iD), J. Puerta Pelayo (iD), I. Redondo (iD), L. Romero, S. Sánchez Navas, L. Urda Gómez (iD), C. Willmott

Universidad Autónoma de Madrid, Madrid, Spain
J.F. de Trocóniz, R. Reyes-Almanza (iD)

Universidad de Oviedo, Instituto Universitario de Ciencias y Tecnologías Espaciales de Asturias (ICTEA), Oviedo, Spain
B. Alvarez Gonzalez (iD), J. Cuevas (iD), C. Erice (iD), J. Fernandez Menendez (iD), S. Folgueras (iD), I. Gonzalez Caballero (iD), J.R. González Fernández, E. Palencia Cortezon (iD), C. Ramón Álvarez, J. Ripoll Sau, V. Rodríguez Bouza (iD), A. Trapote, N. Trevisani (iD)

Instituto de Física de Cantabria (IFCA), CSIC-Universidad de Cantabria, Santander, Spain
J.A. Brochero Cifuentes (iD), I.J. Cabrillo, A. Calderon (iD), J. Duarte Campderros (iD), M. Fernandez (iD), C. Fernandez Madrazo (iD), P.J. Fernández Manteca (iD), A. García Alonso, G. Gomez, C. Martinez Rivero, P. Martinez Ruiz del Arbol (iD), F. Matorras (iD), P. Matorras Cuevas (iD), J. Piedra Gomez (iD), C. Prieels, T. Rodrigo (iD), A. Ruiz-Jimeno (iD), L. Scodellaro (iD), I. Vila, J.M. Vizan Garcia (iD)

University of Colombo, Colombo, Sri Lanka
M.K. Jayananda, B. Kailasapathy[59], D.U.J. Sonnadara, D.D.C. Wickramarathna

University of Ruhuna, Department of Physics, Matara, Sri Lanka
W.G.D. Dharmaratna (iD), K. Liyanage, N. Perera, N. Wickramage

CERN, European Organization for Nuclear Research, Geneva, Switzerland
T.K. Aarrestad (iD), D. Abbaneo, J. Alimena (iD), E. Auffray, G. Auzinger, J. Baechler, P. Baillon[+], D. Barney (iD), J. Bendavid, M. Bianco (iD), A. Bocci (iD), T. Camporesi, M. Capeans Garrido (iD), G. Cerminara, S.S. Chhibra (iD), M. Cipriani (iD), L. Cristella (iD), D. d'Enterria (iD), A. Dabrowski (iD), N. Daci (iD), A. David (iD), A. De Roeck (iD), M.M. Defranchis (iD), M. Deile (iD), M. Dobson, M. Dünser (iD), N. Dupont, A. Elliott-Peisert, N. Emriskova, F. Fallavollita[60], D. Fasanella (iD), S. Fiorendi (iD), A. Florent (iD), G. Franzoni (iD), W. Funk, S. Giani, D. Gigi, K. Gill, F. Glege,

L. Gouskos (iD), M. Haranko (iD), J. Hegeman (iD), Y. Iiyama (iD), V. Innocente (iD), T. James, P. Janot (iD), J. Kaspar (iD), J. Kieseler (iD), M. Komm (iD), N. Kratochwil, C. Lange (iD), S. Laurila, P. Lecoq (iD), K. Long (iD), C. Lourenço (iD), L. Malgeri (iD), S. Mallios, M. Mannelli, A.C. Marini (iD), F. Meijers, S. Mersi (iD), E. Meschi (iD), F. Moortgat (iD), M. Mulders (iD), S. Orfanelli, L. Orsini, F. Pantaleo (iD), L. Pape, E. Perez, M. Peruzzi (iD), A. Petrilli, G. Petrucciani (iD), A. Pfeiffer (iD), M. Pierini (iD), D. Piparo, M. Pitt (iD), H. Qu (iD), T. Quast, D. Rabady (iD), A. Racz, G. Reales Gutiérrez, M. Rieger (iD), M. Rovere, H. Sakulin, J. Salfeld-Nebgen (iD), S. Scarfi, C. Schäfer, C. Schwick, M. Selvaggi (iD), A. Sharma, P. Silva (iD), W. Snoeys (iD), P. Sphicas[61] (iD), S. Summers (iD), V.R. Tavolaro (iD), D. Treille, A. Tsirou, G.P. Van Onsem (iD), M. Verzetti (iD), J. Wanczyk[62], K.A. Wozniak, W.D. Zeuner

Paul Scherrer Institut, Villigen, Switzerland
L. Caminada[63] (iD), A. Ebrahimi (iD), W. Erdmann, R. Horisberger, Q. Ingram, H.C. Kaestli, D. Kotlinski, U. Langenegger, M. Missiroli (iD), T. Rohe

ETH Zurich - Institute for Particle Physics and Astrophysics (IPA), Zurich, Switzerland
K. Androsov[62] (iD), M. Backhaus (iD), P. Berger, A. Calandri (iD), N. Chernyavskaya (iD), A. De Cosa, G. Dissertori (iD), M. Dittmar, M. Donegà, C. Dorfer (iD), F. Eble, K. Gedia, F. Glessgen, T.A. Gómez Espinosa (iD), C. Grab (iD), D. Hits, W. Lustermann, A.-M. Lyon, R.A. Manzoni (iD), C. Martin Perez, M.T. Meinhard, F. Nessi-Tedaldi, J. Niedziela (iD), F. Pauss, V. Perovic, S. Pigazzini (iD), M.G. Ratti (iD), M. Reichmann, C. Reissel, T. Reitenspiess, B. Ristic (iD), D. Ruini, D.A. Sanz Becerra (iD), M. Schönenberger (iD), V. Stampf, J. Steggemann[62] (iD), R. Wallny (iD), D.H. Zhu

Universität Zürich, Zurich, Switzerland
C. Amsler[64] (iD), P. Bärtschi, C. Botta (iD), D. Brzhechko, M.F. Canelli (iD), K. Cormier, A. De Wit (iD), R. Del Burgo, J.K. Heikkilä (iD), M. Huwiler, A. Jofrehei (iD), B. Kilminster (iD), S. Leontsinis (iD), A. Macchiolo (iD), P. Meiring, V.M. Mikuni (iD), U. Molinatti, I. Neutelings, A. Reimers, P. Robmann, S. Sanchez Cruz (iD), K. Schweiger (iD), Y. Takahashi (iD)

National Central University, Chung-Li, Taiwan
C. Adloff[65], C.M. Kuo, W. Lin, A. Roy (iD), T. Sarkar[35] (iD), S.S. Yu

National Taiwan University (NTU), Taipei, Taiwan
L. Ceard, Y. Chao, K.F. Chen (iD), P.H. Chen (iD), W.-S. Hou (iD), Y.y. Li, R.-S. Lu, E. Paganis (iD), A. Psallidas, A. Steen, H.y. Wu, E. Yazgan (iD), P.r. Yu

Chulalongkorn University, Faculty of Science, Department of Physics, Bangkok, Thailand
B. Asavapibhop (iD), C. Asawatangtrakuldee (iD), N. Srimanobhas (iD)

Çukurova University, Physics Department, Science and Art Faculty, Adana, Turkey
F. Boran (iD), S. Damarseckin[66], Z.S. Demiroglu (iD), F. Dolek (iD), I. Dumanoglu[67] (iD), E. Eskut, Y. Guler (iD), E. Gurpinar Guler[68] (iD), I. Hos[69], C. Isik, O. Kara, A. Kayis Topaksu, U. Kiminsu (iD), G. Onengut, K. Ozdemir[70], A. Polatoz, A.E. Simsek (iD), B. Tali[71], U.G. Tok (iD), S. Turkcapar, I.S. Zorbakir (iD), C. Zorbilmez

Middle East Technical University, Physics Department, Ankara, Turkey
B. Isildak[72], G. Karapinar[73], K. Ocalan[74] (iD), M. Yalvac[75] (iD)

Bogazici University, Istanbul, Turkey
B. Akgun, I.O. Atakisi (iD), E. Gülmez (iD), M. Kaya[76] (iD), O. Kaya[77], Ö. Özçelik, S. Tekten[78], E.A. Yetkin[79] (iD)

Istanbul Technical University, Istanbul, Turkey

A. Cakir [iD], K. Cankocak[67] [iD], Y. Komurcu, S. Sen[80] [iD]

Istanbul University, Istanbul, Turkey
S. Cerci[71], B. Kaynak, S. Ozkorucuklu, D. Sunar Cerci[71] [iD]

Institute for Scintillation Materials of National Academy of Science of Ukraine, Kharkov, Ukraine
B. Grynyov

National Scientific Center, Kharkov Institute of Physics and Technology, Kharkov, Ukraine
L. Levchuk [iD]

University of Bristol, Bristol, United Kingdom
D. Anthony, E. Bhal [iD], S. Bologna, J.J. Brooke [iD], A. Bundock [iD], E. Clement [iD], D. Cussans [iD], H. Flacher [iD], J. Goldstein [iD], G.P. Heath, H.F. Heath [iD], M.-L. Holmberg[81], L. Kreczko [iD], B. Krikler [iD], S. Paramesvaran, S. Seif El Nasr-Storey, V.J. Smith, N. Stylianou[82] [iD], K. Walkingshaw Pass, R. White

Rutherford Appleton Laboratory, Didcot, United Kingdom
K.W. Bell, A. Belyaev[83] [iD], C. Brew [iD], R.M. Brown, D.J.A. Cockerill, C. Cooke, K.V. Ellis, K. Harder, S. Harper, J. Linacre [iD], K. Manolopoulos, D.M. Newbold [iD], E. Olaiya, D. Petyt, T. Reis [iD], T. Schuh, C.H. Shepherd-Themistocleous, I.R. Tomalin, T. Williams [iD]

Imperial College, London, United Kingdom
R. Bainbridge [iD], P. Bloch [iD], S. Bonomally, J. Borg [iD], S. Breeze, O. Buchmuller, V. Cepaitis [iD], G.S. Chahal[84] [iD], D. Colling, P. Dauncey [iD], G. Davies [iD], M. Della Negra [iD], S. Fayer, G. Fedi [iD], G. Hall [iD], M.H. Hassanshahi, G. Iles, J. Langford, L. Lyons, A.-M. Magnan, S. Malik, A. Martelli [iD], D.G. Monk, J. Nash[85] [iD], M. Pesaresi, D.M. Raymond, A. Richards, A. Rose, E. Scott [iD], C. Seez, A. Shtipliyski, A. Tapper [iD], K. Uchida, T. Virdee[18] [iD], M. Vojinovic [iD], N. Wardle [iD], S.N. Webb [iD], D. Winterbottom, A.G. Zecchinelli

Brunel University, Uxbridge, United Kingdom
K. Coldham, J.E. Cole [iD], A. Khan, P. Kyberd [iD], I.D. Reid [iD], L. Teodorescu, S. Zahid [iD]

Baylor University, Waco, Texas, USA
S. Abdullin [iD], A. Brinkerhoff [iD], B. Caraway [iD], J. Dittmann [iD], K. Hatakeyama [iD], A.R. Kanuganti, B. McMaster [iD], N. Pastika, M. Saunders [iD], S. Sawant, C. Sutantawibul, J. Wilson [iD]

Catholic University of America, Washington, DC, USA
R. Bartek [iD], A. Dominguez [iD], R. Uniyal [iD], A.M. Vargas Hernandez

The University of Alabama, Tuscaloosa, Alabama, USA
A. Buccilli [iD], S.I. Cooper [iD], D. Di Croce [iD], S.V. Gleyzer [iD], C. Henderson [iD], C.U. Perez [iD], P. Rumerio[86] [iD], C. West [iD]

Boston University, Boston, Massachusetts, USA
A. Akpinar [iD], A. Albert [iD], D. Arcaro [iD], C. Cosby [iD], Z. Demiragli [iD], E. Fontanesi, D. Gastler, J. Rohlf [iD], K. Salyer [iD], D. Sperka, D. Spitzbart [iD], I. Suarez [iD], A. Tsatsos, S. Yuan, D. Zou

Brown University, Providence, Rhode Island, USA
G. Benelli [iD], B. Burkle [iD], X. Coubez[19], D. Cutts [iD], M. Hadley [iD], U. Heintz [iD], J.M. Hogan[87] [iD], G. Landsberg [iD], K.T. Lau [iD], M. Lukasik, J. Luo [iD], M. Narain, S. Sagir[88] [iD], E. Usai [iD], W.Y. Wong, X. Yan [iD], D. Yu [iD], W. Zhang

University of California, Davis, Davis, California, USA

J. Bonilla, C. Brainerd, R. Breedon, M. Calderon De La Barca Sanchez, M. Chertok, J. Conway, P.T. Cox, R. Erbacher, G. Haza, F. Jensen, O. Kukral, R. Lander, M. Mulhearn, D. Pellett, B. Regnery, D. Taylor, Y. Yao, F. Zhang

University of California, Los Angeles, California, USA
M. Bachtis, R. Cousins, A. Datta, D. Hamilton, J. Hauser, M. Ignatenko, M.A. Iqbal, T. Lam, W.A. Nash, S. Regnard, D. Saltzberg, B. Stone, V. Valuev

University of California, Riverside, Riverside, California, USA
K. Burt, Y. Chen, R. Clare, J.W. Gary, M. Gordon, G. Hanson, G. Karapostoli, O.R. Long, N. Manganelli, M. Olmedo Negrete, W. Si, S. Wimpenny, Y. Zhang

University of California, San Diego, La Jolla, California, USA
J.G. Branson, P. Chang, S. Cittolin, S. Cooperstein, N. Deelen, D. Diaz, J. Duarte, R. Gerosa, L. Giannini, D. Gilbert, J. Guiang, R. Kansal, V. Krutelyov, R. Lee, J. Letts, M. Masciovecchio, S. May, M. Pieri, B.V. Sathia Narayanan, V. Sharma, M. Tadel, A. Vartak, F. Würthwein, Y. Xiang, A. Yagil

University of California, Santa Barbara - Department of Physics, Santa Barbara, California, USA
N. Amin, C. Campagnari, M. Citron, A. Dorsett, V. Dutta, J. Incandela, M. Kilpatrick, J. Kim, B. Marsh, H. Mei, M. Oshiro, M. Quinnan, J. Richman, U. Sarica, J. Sheplock, D. Stuart, S. Wang

California Institute of Technology, Pasadena, California, USA
A. Bornheim, O. Cerri, I. Dutta, J.M. Lawhorn, N. Lu, J. Mao, H.B. Newman, J. Ngadiuba, T.Q. Nguyen, M. Spiropulu, J.R. Vlimant, C. Wang, S. Xie, Z. Zhang, R.Y. Zhu

Carnegie Mellon University, Pittsburgh, Pennsylvania, USA
J. Alison, S. An, M.B. Andrews, P. Bryant, T. Ferguson, A. Harilal, C. Liu, T. Mudholkar, M. Paulini, A. Sanchez

University of Colorado Boulder, Boulder, Colorado, USA
J.P. Cumalat, W.T. Ford, A. Hassani, E. MacDonald, R. Patel, A. Perloff, C. Savard, K. Stenson, K.A. Ulmer, S.R. Wagner

Cornell University, Ithaca, New York, USA
J. Alexander, S. Bright-Thonney, Y. Cheng, D.J. Cranshaw, S. Hogan, J. Monroy, J.R. Patterson, D. Quach, J. Reichert, M. Reid, A. Ryd, W. Sun, J. Thom, P. Wittich, R. Zou

Fermi National Accelerator Laboratory, Batavia, Illinois, USA
M. Albrow, M. Alyari, G. Apollinari, A. Apresyan, A. Apyan, S. Banerjee, L.A.T. Bauerdick, D. Berry, J. Berryhill, P.C. Bhat, K. Burkett, J.N. Butler, A. Canepa, G.B. Cerati, H.W.K. Cheung, F. Chlebana, M. Cremonesi, K.F. Di Petrillo, V.D. Elvira, Y. Feng, J. Freeman, Z. Gecse, L. Gray, D. Green, S. Grünendahl, O. Gutsche, R.M. Harris, R. Heller, T.C. Herwig, J. Hirschauer, B. Jayatilaka, S. Jindariani, M. Johnson, U. Joshi, T. Klijnsma, B. Klima, K.H.M. Kwok, S. Lammel, D. Lincoln, R. Lipton, T. Liu, C. Madrid, K. Maeshima, C. Mantilla, D. Mason, P. McBride, P. Merkel, S. Mrenna, S. Nahn, V. O'Dell, V. Papadimitriou, K. Pedro, C. Pena[56], O. Prokofyev, F. Ravera, A. Reinsvold Hall, L. Ristori, B. Schneider, E. Sexton-Kennedy, N. Smith, A. Soha, W.J. Spalding, L. Spiegel, S. Stoynev, J. Strait, L. Taylor, S. Tkaczyk, N.V. Tran, L. Uplegger, E.W. Vaandering, H.A. Weber

48

University of Florida, Gainesville, Florida, USA
D. Acosta (iD), P. Avery, D. Bourilkov (iD), L. Cadamuro (iD), V. Cherepanov, F. Errico (iD), R.D. Field, D. Guerrero, B.M. Joshi (iD), M. Kim, E. Koenig, J. Konigsberg (iD), A. Korytov, K.H. Lo, K. Matchev (iD), N. Menendez (iD), G. Mitselmakher (iD), A. Muthirakalayil Madhu, N. Rawal, D. Rosenzweig, S. Rosenzweig, K. Shi (iD), J. Sturdy (iD), J. Wang (iD), E. Yigitbasi (iD), X. Zuo

Florida State University, Tallahassee, Florida, USA
T. Adams (iD), A. Askew (iD), R. Habibullah (iD), V. Hagopian, K.F. Johnson, R. Khurana, T. Kolberg (iD), G. Martinez, H. Prosper (iD), C. Schiber, O. Viazlo (iD), R. Yohay (iD), J. Zhang

Florida Institute of Technology, Melbourne, Florida, USA
M.M. Baarmand (iD), S. Butalla, T. Elkafrawy[89] (iD), M. Hohlmann (iD), R. Kumar Verma (iD), D. Noonan (iD), M. Rahmani, F. Yumiceva (iD)

University of Illinois at Chicago (UIC), Chicago, Illinois, USA
M.R. Adams, H. Becerril Gonzalez (iD), R. Cavanaugh (iD), X. Chen (iD), S. Dittmer, O. Evdokimov (iD), C.E. Gerber (iD), D.A. Hangal (iD), D.J. Hofman (iD), A.H. Merrit, C. Mills (iD), G. Oh (iD), T. Roy, S. Rudrabhatla, M.B. Tonjes (iD), N. Varelas (iD), J. Viinikainen (iD), X. Wang, Z. Wu (iD), Z. Ye (iD)

The University of Iowa, Iowa City, Iowa, USA
M. Alhusseini (iD), K. Dilsiz[90] (iD), R.P. Gandrajula (iD), O.K. Köseyan (iD), J.-P. Merlo, A. Mestvirishvili[91], J. Nachtman, H. Ogul[92] (iD), Y. Onel (iD), A. Penzo, C. Snyder, E. Tiras[93] (iD)

Johns Hopkins University, Baltimore, Maryland, USA
O. Amram (iD), B. Blumenfeld (iD), L. Corcodilos (iD), J. Davis, M. Eminizer (iD), A.V. Gritsan (iD), S. Kyriacou, P. Maksimovic (iD), J. Roskes (iD), M. Swartz, T.Á. Vámi (iD)

The University of Kansas, Lawrence, Kansas, USA
A. Abreu, J. Anguiano, C. Baldenegro Barrera (iD), P. Baringer (iD), A. Bean (iD), A. Bylinkin (iD), Z. Flowers, T. Isidori, S. Khalil (iD), J. King, G. Krintiras (iD), A. Kropivnitskaya (iD), M. Lazarovits, C. Lindsey, J. Marquez, N. Minafra (iD), M. Murray (iD), M. Nickel, C. Rogan (iD), C. Royon, R. Salvatico (iD), S. Sanders, E. Schmitz, C. Smith (iD), J.D. Tapia Takaki (iD), Q. Wang (iD), Z. Warner, J. Williams (iD), G. Wilson (iD)

Kansas State University, Manhattan, Kansas, USA
S. Duric, A. Ivanov (iD), K. Kaadze (iD), D. Kim, Y. Maravin (iD), T. Mitchell, A. Modak, K. Nam

Lawrence Livermore National Laboratory, Livermore, California, USA
F. Rebassoo, D. Wright

University of Maryland, College Park, Maryland, USA
E. Adams, A. Baden, O. Baron, A. Belloni (iD), S.C. Eno (iD), N.J. Hadley (iD), S. Jabeen (iD), R.G. Kellogg, T. Koeth, A.C. Mignerey, S. Nabili, M. Seidel (iD), A. Skuja (iD), L. Wang, K. Wong (iD)

Massachusetts Institute of Technology, Cambridge, Massachusetts, USA
D. Abercrombie, G. Andreassi, R. Bi, S. Brandt, W. Busza (iD), I.A. Cali, Y. Chen (iD), M. D'Alfonso (iD), J. Eysermans, C. Freer (iD), G. Gomez Ceballos, M. Goncharov, P. Harris, M. Hu, M. Klute (iD), D. Kovalskyi (iD), J. Krupa, Y.-J. Lee (iD), B. Maier, C. Mironov (iD), C. Paus (iD), D. Rankin (iD), C. Roland (iD), G. Roland, Z. Shi (iD), G.S.F. Stephans (iD), K. Tatar (iD), J. Wang, Z. Wang (iD), B. Wyslouch (iD)

University of Minnesota, Minneapolis, Minnesota, USA
R.M. Chatterjee, A. Evans (iD), P. Hansen, J. Hiltbrand, Sh. Jain (iD), M. Krohn, Y. Kubota, J. Mans (iD), M. Revering, R. Rusack (iD), R. Saradhy, N. Schroeder (iD), N. Strobbe (iD), M.A. Wadud

University of Nebraska-Lincoln, Lincoln, Nebraska, USA

K. Bloom, M. Bryson, S. Chauhan, D.R. Claes, C. Fangmeier, L. Finco, F. Golf, C. Joo, I. Kravchenko, M. Musich, I. Reed, J.E. Siado, G.R. Snow†, W. Tabb, F. Yan

State University of New York at Buffalo, Buffalo, New York, USA

G. Agarwal, H. Bandyopadhyay, L. Hay, I. Iashvili, A. Kharchilava, C. McLean, D. Nguyen, J. Pekkanen, S. Rappoccio, A. Williams

Northeastern University, Boston, Massachusetts, USA

G. Alverson, E. Barberis, Y. Haddad, A. Hortiangtham, J. Li, G. Madigan, B. Marzocchi, D.M. Morse, V. Nguyen, T. Orimoto, A. Parker, L. Skinnari, A. Tishelman-Charny, T. Wamorkar, B. Wang, A. Wisecarver, D. Wood

Northwestern University, Evanston, Illinois, USA

S. Bhattacharya, J. Bueghly, Z. Chen, A. Gilbert, T. Gunter, K.A. Hahn, Y. Liu, N. Odell, M.H. Schmitt, M. Velasco

University of Notre Dame, Notre Dame, Indiana, USA

R. Band, R. Bucci, A. Das, N. Dev, R. Goldouzian, M. Hildreth, K. Hurtado Anampa, C. Jessop, K. Lannon, J. Lawrence, N. Loukas, D. Lutton, N. Marinelli, I. Mcalister, T. McCauley, F. Meng, K. Mohrman, Y. Musienko[48], R. Ruchti, P. Siddireddy, A. Townsend, M. Wayne, A. Wightman, M. Wolf, M. Zarucki, L. Zygala

The Ohio State University, Columbus, Ohio, USA

B. Bylsma, B. Cardwell, L.S. Durkin, B. Francis, C. Hill, M. Nunez Ornelas, K. Wei, B.L. Winer, B.R. Yates

Princeton University, Princeton, New Jersey, USA

F.M. Addesa, B. Bonham, P. Das, G. Dezoort, P. Elmer, A. Frankenthal, B. Greenberg, N. Haubrich, S. Higginbotham, A. Kalogeropoulos, G. Kopp, S. Kwan, D. Lange, M.T. Lucchini, D. Marlow, K. Mei, I. Ojalvo, J. Olsen, C. Palmer, D. Stickland, C. Tully

University of Puerto Rico, Mayaguez, Puerto Rico, USA

S. Malik, S. Norberg

Purdue University, West Lafayette, Indiana, USA

A.S. Bakshi, V.E. Barnes, R. Chawla, S. Das, L. Gutay, M. Jones, A.W. Jung, S. Karmarkar, M. Liu, G. Negro, N. Neumeister, G. Paspalaki, C.C. Peng, S. Piperov, A. Purohit, J.F. Schulte, M. Stojanovic[15], J. Thieman, F. Wang, R. Xiao, W. Xie

Purdue University Northwest, Hammond, Indiana, USA

J. Dolen, N. Parashar

Rice University, Houston, Texas, USA

A. Baty, M. Decaro, S. Dildick, K.M. Ecklund, S. Freed, P. Gardner, F.J.M. Geurts, A. Kumar, W. Li, B.P. Padley, R. Redjimi, W. Shi, A.G. Stahl Leiton, S. Yang, L. Zhang, Y. Zhang

University of Rochester, Rochester, New York, USA

A. Bodek, P. de Barbaro, R. Demina, J.L. Dulemba, C. Fallon, T. Ferbel, M. Galanti, A. Garcia-Bellido, O. Hindrichs, A. Khukhunaishvili, E. Ranken, R. Taus

Rutgers, The State University of New Jersey, Piscataway, New Jersey, USA

B. Chiarito, J.P. Chou, A. Gandrakota, Y. Gershtein, E. Halkiadakis, A. Hart,

M. Heindl, O. Karacheban[22], I. Laflotte, A. Lath, R. Montalvo, K. Nash, M. Osherson, S. Salur, S. Schnetzer, S. Somalwar, R. Stone, S.A. Thayil, S. Thomas, H. Wang

University of Tennessee, Knoxville, Tennessee, USA
H. Acharya, A.G. Delannoy, S. Spanier

Texas A&M University, College Station, Texas, USA
O. Bouhali[94], M. Dalchenko, A. Delgado, R. Eusebi, J. Gilmore, T. Huang, T. Kamon[95], H. Kim, S. Luo, S. Malhotra, R. Mueller, D. Overton, D. Rathjens, A. Safonov

Texas Tech University, Lubbock, Texas, USA
N. Akchurin, J. Damgov, V. Hegde, S. Kunori, K. Lamichhane, S.W. Lee, T. Mengke, S. Muthumuni, T. Peltola, I. Volobouev, Z. Wang, A. Whitbeck

Vanderbilt University, Nashville, Tennessee, USA
E. Appelt, S. Greene, A. Gurrola, W. Johns, A. Melo, H. Ni, K. Padeken, F. Romeo, P. Sheldon, S. Tuo, J. Velkovska

University of Virginia, Charlottesville, Virginia, USA
M.W. Arenton, B. Cox, G. Cummings, J. Hakala, R. Hirosky, M. Joyce, A. Ledovskoy, A. Li, C. Neu, B. Tannenwald, S. White, E. Wolfe

Wayne State University, Detroit, Michigan, USA
N. Poudyal

University of Wisconsin - Madison, Madison, WI, Wisconsin, USA
K. Black, T. Bose, J. Buchanan, C. Caillol, S. Dasu, I. De Bruyn, P. Everaerts, F. Fienga, C. Galloni, H. He, M. Herndon, A. Hervé, U. Hussain, A. Lanaro, A. Loeliger, R. Loveless, J. Madhusudanan Sreekala, A. Mallampalli, A. Mohammadi, D. Pinna, A. Savin, V. Shang, V. Sharma, W.H. Smith, D. Teague, S. Trembath-Reichert, W. Vetens

†: Deceased
1: Also at TU Wien, Wien, Austria
2: Also at Institute of Basic and Applied Sciences, Faculty of Engineering, Arab Academy for Science, Technology and Maritime Transport, Alexandria, Egypt
3: Also at Université Libre de Bruxelles, Bruxelles, Belgium
4: Also at Universidade Estadual de Campinas, Campinas, Brazil
5: Also at Federal University of Rio Grande do Sul, Porto Alegre, Brazil
6: Also at University of Chinese Academy of Sciences, Beijing, China
7: Also at Department of Physics, Tsinghua University, Beijing, China
8: Also at UFMS, Nova Andradina, Brazil
9: Also at Nanjing Normal University Department of Physics, Nanjing, China
10: Now at The University of Iowa, Iowa City, Iowa, USA
11: Also at Institute for Theoretical and Experimental Physics named by A.I. Alikhanov of NRC 'Kurchatov Institute', Moscow, Russia
12: Also at Joint Institute for Nuclear Research, Dubna, Russia
13: Also at Cairo University, Cairo, Egypt
14: Also at Zewail City of Science and Technology, Zewail, Egypt
15: Also at Purdue University, West Lafayette, Indiana, USA
16: Also at Université de Haute Alsace, Mulhouse, France
17: Also at Erzincan Binali Yildirim University, Erzincan, Turkey
18: Also at CERN, European Organization for Nuclear Research, Geneva, Switzerland
19: Also at RWTH Aachen University, III. Physikalisches Institut A, Aachen, Germany

20: Also at University of Hamburg, Hamburg, Germany

21: Also at Isfahan University of Technology, Isfahan, Iran

22: Also at Brandenburg University of Technology, Cottbus, Germany

23: Also at Skobeltsyn Institute of Nuclear Physics, Lomonosov Moscow State University, Moscow, Russia

24: Also at Physics Department, Faculty of Science, Assiut University, Assiut, Egypt

25: Also at Karoly Robert Campus, MATE Institute of Technology, Gyongyos, Hungary

26: Also at Institute of Physics, University of Debrecen, Debrecen, Hungary

27: Also at Institute of Nuclear Research ATOMKI, Debrecen, Hungary

28: Also at MTA-ELTE Lendület CMS Particle and Nuclear Physics Group, Eötvös Loránd University, Budapest, Hungary

29: Also at Wigner Research Centre for Physics, Budapest, Hungary

30: Also at IIT Bhubaneswar, Bhubaneswar, India

31: Also at Institute of Physics, Bhubaneswar, India

32: Also at G.H.G. Khalsa College, Punjab, India

33: Also at Shoolini University, Solan, India

34: Also at University of Hyderabad, Hyderabad, India

35: Also at University of Visva-Bharati, Santiniketan, India

36: Also at Indian Institute of Technology (IIT), Mumbai, India

37: Also at Deutsches Elektronen-Synchrotron, Hamburg, Germany

38: Also at Sharif University of Technology, Tehran, Iran

39: Also at Department of Physics, University of Science and Technology of Mazandaran, Behshahr, Iran

40: Now at INFN Sezione di Bari, Università di Bari, Politecnico di Bari, Bari, Italy

41: Also at Italian National Agency for New Technologies, Energy and Sustainable Economic Development, Bologna, Italy

42: Also at Centro Siciliano di Fisica Nucleare e di Struttura Della Materia, Catania, Italy

43: Also at Università di Napoli 'Federico II', Napoli, Italy

44: Also at Consiglio Nazionale delle Ricerche - Istituto Officina dei Materiali, PERUGIA, Italy

45: Also at Riga Technical University, Riga, Latvia

46: Also at Consejo Nacional de Ciencia y Tecnología, Mexico City, Mexico

47: Also at IRFU, CEA, Université Paris-Saclay, Gif-sur-Yvette, France

48: Also at Institute for Nuclear Research, Moscow, Russia

49: Now at National Research Nuclear University 'Moscow Engineering Physics Institute' (MEPhI), Moscow, Russia

50: Also at Institute of Nuclear Physics of the Uzbekistan Academy of Sciences, Tashkent, Uzbekistan

51: Also at St. Petersburg State Polytechnical University, St. Petersburg, Russia

52: Also at University of Florida, Gainesville, Florida, USA

53: Also at Imperial College, London, United Kingdom

54: Also at Moscow Institute of Physics and Technology, Moscow, Russia

55: Also at P.N. Lebedev Physical Institute, Moscow, Russia

56: Also at California Institute of Technology, Pasadena, California, USA

57: Also at Budker Institute of Nuclear Physics, Novosibirsk, Russia

58: Also at Faculty of Physics, University of Belgrade, Belgrade, Serbia

59: Also at Trincomalee Campus, Eastern University, Sri Lanka, Nilaveli, Sri Lanka

60: Also at INFN Sezione di Pavia, Università di Pavia, Pavia, Italy

61: Also at National and Kapodistrian University of Athens, Athens, Greece

62: Also at Ecole Polytechnique Fédérale Lausanne, Lausanne, Switzerland

63: Also at Universität Zürich, Zurich, Switzerland
64: Also at Stefan Meyer Institute for Subatomic Physics, Vienna, Austria
65: Also at Laboratoire d'Annecy-le-Vieux de Physique des Particules, IN2P3-CNRS, Annecy-le-Vieux, France
66: Also at Şırnak University, Sirnak, Turkey
67: Also at Near East University, Research Center of Experimental Health Science, Nicosia, Turkey
68: Also at Konya Technical University, Konya, Turkey
69: Also at Istanbul University - Cerrahpasa, Faculty of Engineering, Istanbul, Turkey
70: Also at Piri Reis University, Istanbul, Turkey
71: Also at Adiyaman University, Adiyaman, Turkey
72: Also at Ozyegin University, Istanbul, Turkey
73: Also at Izmir Institute of Technology, Izmir, Turkey
74: Also at Necmettin Erbakan University, Konya, Turkey
75: Also at Bozok Universitetesi Rektörlügü, Yozgat, Turkey
76: Also at Marmara University, Istanbul, Turkey
77: Also at Milli Savunma University, Istanbul, Turkey
78: Also at Kafkas University, Kars, Turkey
79: Also at Istanbul Bilgi University, Istanbul, Turkey
80: Also at Hacettepe University, Ankara, Turkey
81: Also at Rutherford Appleton Laboratory, Didcot, United Kingdom
82: Also at Vrije Universiteit Brussel, Brussel, Belgium
83: Also at School of Physics and Astronomy, University of Southampton, Southampton, United Kingdom
84: Also at IPPP Durham University, Durham, United Kingdom
85: Also at Monash University, Faculty of Science, Clayton, Australia
86: Also at Università di Torino, Torino, Italy
87: Also at Bethel University, St. Paul, Minneapolis, USA
88: Also at Karamanoğlu Mehmetbey University, Karaman, Turkey
89: Also at Ain Shams University, Cairo, Egypt
90: Also at Bingol University, Bingol, Turkey
91: Also at Georgian Technical University, Tbilisi, Georgia
92: Also at Sinop University, Sinop, Turkey
93: Also at Erciyes University, Kayseri, Turkey
94: Also at Texas A&M University at Qatar, Doha, Qatar
95: Also at Kyungpook National University, Daegu, Korea